JAERI-M
8739

SENSITIVITY ANALYSIS OF NEUTRONICS CALCULATIONS IN THE PRELIMINARY DESIGN OF JAERI EXPERIMENTAL FUSION REACTOR

(Revised)

March 1980

Michinori YAMAUCHI*, Yasushi SEKI and Hiromasa IIDA

日本原子力研究所
Japan Atomic Energy Research Institute

この報告書は，日本原子力研究所が JAERI-M レポートとして，不定期に刊行している研究報告書です．入手，複製などのお問合わせは，日本原子力研究所技術情報部（茨城県那珂郡東海村）あて，お申しこしください．

JAERI-M reports, issued irregularly, describe the results of research works carried out in JAERI. Inquiries about the availability of reports and their reproduction should be addressed to Division of Technical Information, Japan Atomic Energy Research Institute, Tokai-mura, Naka-gun, Ibaraki-ken, Japan.

JAERI -M 8739

Sensitivity Analysis of Neutronics Calculations in the Preliminary Design of JAERI Experimental Fusion Reactor (Revised)

Michinori YAMAUCHI*, Yasushi SEKI and Hiromasa IIDA

Division of Thermonuclear Fusion Research
Tokai Research Establishment, JAERI

(Received January 31, 1980)

Sensitivity of principal neutronics characteristic quantities for the neutron cross sections of JAERI Experimental Fusion Reactor (JXFR) has been studied by means of sensitivity analysis method based on linear perturbation theory. The same study was made previously. After publication of the previous results, however, the SWANLAKE code used to calculate sensitivities was found to include error derived during its conversion process. The study was thus repeated with corrected SWANLAKE. The quantities studied are calculational results for the first preliminary design of JXFR such as the (n,p) reaction rates of ^{58}Ni and ^{54}Fe in the outer part of superconducting toroidal field coil (TFC), the copper atomic displacement rate in the inner part of TFC and the tritium production rate in the outer blanket. Though the calculational results do not contradict essentially the results in the former study, the newly calculated sensitivities were found to be more or less different from the previous ones. Therefore, the results and discussion of analysis given in this report are revised, with the values corrected. The errors of the (n,p) reaction rates and the copper displacement rate due to the uncertainties of cross sections were estimated to be about 50-70% and 25-65%, respectively, taking into account the direct sensitivity of (n,p) reaction cross sections in the former.

Keywords: Linear Perturbation, Sensitivity Analysis, Uncertainty Evaluation, JAERI Experimental Fusion Reactor, Superconducting Magnet, Blanket, Total Cross Section, (n,p) Reaction Rate, Nickel 58, Iron 54, Copper Displacement Rate, Tritium Breeding Ratio, Sn Approximation

*) Tokyo Shibaura Electric Co., Ltd., Tokyo, Japan

JAERI－M 8739

感度解析による核融合実験炉核計算精度の検討（改訂版）

日本原子力研究所東海研究所核融合研究部
山内通則＊・関　泰・飯田浩正

（1980年1月31日受理）

1次摂動理論に基づく感度解析法を導入し，核融合実験炉JXFRの構成材料の断面積に対する主要な核特性値の感度を解析した。同種の報告がすでに以前なされているが，その後の検討で使用した感度計算コードSWANLAKEに変換の際に生じたプログラムエラーのあることが判明したので，それを修正し，主要な内容について再計算を行なった。対象とした特性値は，JXFRの第1次予備設計における計算結果の一部であり，超電導トロイダルコイルの外側部分の（n，p）反応率，超電導コイルの内側部分の銅原子はじき出し率およびリチウム領域のトリチウム生成反応率である。再計算の結果は前回得られた評価の大要を打ち消すものではないが，計算値に多少の違いが生じたので，値を修正するとともに，それに基づく評価の内容も更新した。感度計算値の修正の結果，反応率を計算するための応答関数も含めた断面積の不確かさに起因する（n，p）反応率と銅原子はじき出し率の誤差は，それぞれ約50～70%，25～65%と大きくなり，それだけ断面積精度に対する要求が増大したといえる。

＊）　外来研究員：東京芝浦電気（株）

CONTENTS

目　　次

1. INTRODUCTION

A sensitivity study[1] for the cross sections of JAERI Experimental Fusion Reactor (JXFR)[2] was reported. A linear perturbation code SWANLAKE[3] was used in the work. On the succeeding utilization of the code, a program error which had occurred during the program conversion process from IBM machine to FACOM 230/75 in JAERI was found out. Accordingly perturbation calculations for principal cases were repeated using the revised version of SWANLAKE code to reassess results of the former work. As a result, the general outline of the former work turned out to be correct. But most of sensitivity coefficients became greater than those obtained in the former work by about a factor of 3. In this report newly obtained calculational results are described and some important discussions are given.

Sensitivities of the following quantities are studied : (1) (n,p) reaction rates of ^{58}Ni and ^{54}Fe in the outer part of the superconducting toroidal field coil (TFC), (2) Cu atomic displacement rate at the nearest portion to the plasma in the inner part of the TFC and (3) tritium production rate in the outer blanket. The first contributes most to the spatial dose rate arround the reactor a few days after the shutdown. The second is the limiting condition induced by irradiation in the inner part of the TFC. These two sensitivity studies were performed to investigate the reaction rate inaccuracies due to cross section uncertainties in the case of deep penetration problems. The third was carried out because the tritium breeding is one of the most important functions of the outer blanket.

The calculational method is briefly described in Section 2 and the calculated results are given in Section 3. Dependence of sensitivities on the order of Sn and the error estimation are discussed in Section 4. The dependence on Sn order which was unacceptably large in the previous report[1] turned out to be small enough. The method of the error estimation was modified a little. That is, while the full correlation was supposed in the former work, the estimation under the condition of no correlation was added. Lastly main results are summarized in Section 5.

2. OUTLINE OF CALCULATIONAL METHOD

The one dimensional calculational models of JXFR are shown in Table 2.1 and 2.2 for the outer and inner models, respectively. Neutron mean free paths for 4 energy groups are also shown in the tables to be compared with the mesh intervals used in this study. Models are same as the standard models used in the previous work[1] and also in the first preliminary design of JXFR.[2] Detailed discussions concerning mesh intervals and so forth are already given.[1] The forward transport calculation was performed with the model in Table 2.1 setting 14 MeV neutron source in the plasma region for the sensitivity study of the activation reaction rate in the outer part of the TFC. In the case of adjoint calculation, the activation reaction cross sections were placed in every interval of the TFC. For the sensitivity study of tritium breeding, regions situated beyond the outer boundary of blanket are excluded to save computing time. Macroscopic tritium production cross sections as the adjoint sources were placed in all intervals of Li_2O pebble or block region. The transport calculation for the sensitivity study of copper atomic displacement rate in the innermost part of the TFC were performed with the model in Table 2.2. The displacement cross section was placed as the adjoint source only in the innermost mesh interval of the TFC where the neutron flux is highest in the coil. One dimensional forward and adjoint transport calculation were carried out by the ANISN code[4] with the $S_{16}P_5$ approximation except for a set of forward and adjoint calculations which were carried out with the S_8P_5 appoximations for the discussion of sensitivity change due to the difference of Sn order. The 42-group neutron cross sections from the GICX40 library[5] were used in this work. The 42-energy-group structure is shown in Table 2.3. Profiles of the response functions used in this work are shown in Fig. 2.1. These are $^{6}Li(n,\alpha)T$, $^{7}Li(n,n'\alpha)T$, $^{58}Ni(n,p)$, $^{54}Fe(n,p)$ and Cu displacement cross sections. Mixtures to construct the macroscopic cross sections for the outer blanket, shield and TFC of JXFR are shown in Table 2.4. and those for the inner blanket, shield and TFC are shown in Table 2.5. Sensitivities are calculated by a linear perturbation code SWANLAKE.[3] Important constituents for which responses have large sensitivities are marked in the leftmost column with symbols o and Δ. In the case of (n,p) activation reactions in the outer part of the TFC, the cross sections of ^{6}Li, ^{7}Li, ^{16}O, Mo, Cr, Ni, Fe and H were chosen for the study, and the same set of elements except ^{12}C substituted for H were chosen in the case of tritium production reactions. 13 elements shown in Table 2.5 with a symbol o were selected in the case of copper atomic displacement rate in the inner part of the TFC.

Table 2.1 Calculational Model and Mean Free Paths of Outer Blanket, Shield and TFC

Zone	Region No.	Region	Radius (cm)	Mesh No.	Mesh Width (cm)	Mean Free Paths (cm) G.1[1]	G.18[2]	G.30[3]	G.42[4]
			0	1					
	1	Plasma	150	2	(1) 150	1×10^{11}	2×10^{10}	5×10^{9}	5×10^{9}
	2	Vacuum	174.5	3	(1) 24.5	1×10^{11}	2×10^{10}	5×10^{9}	5×10^{9}
BLANKET	3	Carbon coating	175	5	(2) 0.25	8.9	4.5	2.5	2.5
	4	Stainless Steel	176	7	(2) 0.5	4.6	4.2	1.3	0.92
	5	Li_2O Pebble[5]	195	11	(4) 4.75	18	12	8.2	0.77
	6	Li_2O Block[6]	235	31	(20) 2	6.8	4.4	3.5	0.26
	7	S.S.(90%)+He(10%)	255	47	(16) 1.25	5.1	4.7	1.4	1.0
	8	Stainless Steel	259.5	57	(10) 0.45	4.6	4.2	1.3	0.92
	9	Vacuum	335	58	(1) 75.5	1×10^{11}	2×10^{10}	5×10^{9}	5×10^{9}
SHIELD	10	H.C.+Borated Water[7]	410	108	(50) 1.5	6.6	2.9	1.2	0.75
	11	Lead	415	116	(8) 0.625	6.1	5.8	2.7	2.7
	12	Air	425	117	(1) 10	1×10^{4}	8×10^{3}	2×10^{3}	2×10^{3}
	13	Insulator (Al)	435	119	(2) 5	32	16	36	33
TFC	14	SCM[8]	575	189	(70) 2	4.6	3.9	1.1	1.1
	15	Insulator (Al)	585	191	(2) 5	32	16	36	33

N.B. 1) 15.0 ∿ 13.7 MeV
2) 1.08 ∿ 0.800 MeV
3) 2.15 ∿ 1.00 keV
4) 0.215 ∿ 0.001 eV
5) Li_2O(24%)+S.S(9%)+He(27%)
6) Li_2O(72%)+S.S(17%)+He(11%)
7) Heavy Concrete (90%)+Borated Water(10%)
8) Superconducting Magnet

Table 2.2 Calculational Model and Mean Free Paths of Inner Blanket, Shield and TFC

Zone	Region No.	Region	Radius (cm)	Mesh No.	Mesh Width (cm)	Mean Free Paths (cm) G.1[1]	G.18[2]	G.30[3]	G.42[4]
			0	1					
	1	Plasma	150	2 (1)	150	1×10^{11}	2×10^{10}	5×10^{9}	5×10^{9}
	2	Vacuum	174.5	3 (1)	24.5	1×10^{11}	2×10^{10}	5×10^{9}	5×10^{9}
	3	Carbon Coating	175	5 (2)	0.25	8.9	4.5	2.5	2.5
	4	Stainless Steel	176	7 (2)	0.5	4.6	4.2	1.3	0.92
	5	Helium	181	8 (1)	5	1×10^{4}	2×10^{3}	1×10^{4}	1×10^{4}
BLANKET	6	Stainless Steel	182	10 (2)	0.5	4.6	4.2	1.3	0.92
	7	S.S(90%)+He(10%)	191	20 (10)	0.9	5.1	4.7	1.4	1.0
	8	S.S+W+He[5]	215	44 (24)	1	4.0	3.2	0.65	1.0
	9	Stainless Steel	219	48 (4)	1	4.6	4.2	1.3	0.92
	10	Vacuum	255	49 (1)	36	1×10^{11}	2×10^{10}	5×10^{9}	5×10^{9}
SHIELD	11	H.C.+Borated Water[6]	285	89 (40)	0.75	6.6	2.9	1.2	0.75
	12	S.S+B_4C+H_2O[7]	295	97 (8)	1.25	5.6	3.1	0.75	0.0085
	13	Air	305	98 (1)	10	1×10^{4}	8×10^{3}	2×10^{3}	2×10^{3}
	14	Insulator (Al)	315	100 (2)	5	32	16	36	33
TFC	15	SCM[8]	405	190 (90)	1	4.6	3.9	1.1	1.1
	16	Insulator (Al)	415	192 (2)	5	32	16	36	33

N.B. 1) 15.0 ∿ 13.7 MeV
2) 1.08 ∿ 0.800 MeV
3) 2.15 ∿ 1.00 keV
4) 0.215 ∿ 0.001 eV
5) S.S(17%)+W(73%)+He(10%)
6) Heavy Concrete (90%)+Borated Water (10%)
7) S.S.(40%)+B_4C(40%)+H_2O(20%)
8) Superconducting Magnet

Table 2.3 42-group neutron energy group structure

Group	Energy Limits	Mid-Point Energy	Lethargy Width
1	15.000 – 13.720 MeV	14.360 MeV	0.08920
2	13.720 – 12.549	13.135	0.08921
3	12.549 – 11.478	12.014	0.08921
4	11.478 – 10.500	10.989	0.08906
5	10.500 – 9.314	9.907	0.1199
6	9.314 – 8.261	8.788	0.1200
7	8.261 – 7.328	7.795	0.1198
8	7.328 – 6.500	6.914	0.1199
9	6.500 – 5.757	6.129	0.1214
10	5.757 – 5.099	5.428	0.1214
11	5.099 – 4.516	4.808	0.1214
12	4.516 – 4.000	4.258	0.1213
13	4.000 – 3.162	3.581	0.2351
14	3.162 – 2.500	2.831	0.2349
15	2.500 – 1.871	2.186	0.290
16	1.871 – 1.400	1.636	0.290
17	1.400 – 1.058	1.229	0.280
18	1.058 – 0.800	0.929	0.280
19	0.800 – 0.566	0.683	0.346
20	0.566 – 0.400	0.483	0.347
21	0.400 – 0.283	0.342	0.346
22	0.283 – 0.200	0.242	0.347
23	0.200 – 0.141	0.171	0.350
24	0.141 – 0.100	0.121	0.344
25	100.0 – 46.5 keV	73.25 keV	0.766
26	46.5 – 21.5	34.0	0.771
27	21.5 – 10.0	15.75	0.765
28	10.0 – 4.65	7.325	0.766
29	4.65 – 2.15	3.40	0.771
30	2.15 – 1.00	1.575	0.765
31	1.00 – 0.465	0.733	0.766
32	0.465 – 0.215	0.340	0.771
33	0.215 – 0.100	0.158	0.765
34	100.0 – 46.5 eV	73.25 eV	0.766
35	46.5 – 21.5	34.0	0.771
36	21.5 – 10.0	15.75	0.765
37	10.0 – 4.65	7.325	0.766
38	4.65 – 2.15	3.40	0.771
39	2.15 – 1.00	1.58	0.765
40	1.00 – 0.465	0.733	0.766
41	0.465 – 0.215	0.340	0.771
42	0.215 – 0.001	0.108	—

Table 2.4 Mixtures for Outer Blanket, Shield and TFC of JXFR

(Unit; atoms×10^{24}/cm^3)

SWANLAKE	Element	Plasma Vacuum	Carbon Coating	S.S.	Li_2O(24) SS (9) He (27)	Li_2O(72) S.S.(17) He (11)	S.S.(90) He (10)	H.C. H_2O(B)	Lead	Air	Insulator (Al)	SCM
○	^{6}Li				1.228−3	3.685−3						
○	^{7}Li				1.532−2	4.598−2						
△	^{12}C		8.374−2									
○	^{16}O				8.275−3	2.483−5		3.383−2		1.17−5		
	^{4}He				2.700−5	1.100−5	1.0−5					
	Nb											3.884−3
○	Mo			1.255−3	1.130−4	2.134−4	1.130−3					7.530−4
○	Cr			1.575−2	1.418−3	2.678−3	1.418−2					9.450−3
○	Ni			9.848−3	8.863−4	1.674−3	8.863−3					5.909−3
○	Fe			5.909−2	5.319−3	1.005−2	5.318−2	3.176−2				3.545−2
△	H	1.0−11						1.861−2				
	^{10}B							5.601−5				
	N									4.22−5		
	Al							2.728−3			1.801−2	
	Cu											2.370−2
	Pb								3.296−2			
	Ca							2.155−3				
Total Width(cm)		250	0.5	5.5	19	40	20	75	5	10	20	140

Table 2.5 Mixtures for Inner Blanket, Shield and TFC of JXFR

(Unit : atoms×10^{24}/cm^3)

SWANLAKE	Element	Plasm Vacuum	Carbona Coating	S.S.	He	S.S.(90) He (10)	S.S.(17) W (73) He (10)	H.C. H_2O(B)	S.S.(40) B_4C (40) H_2O (20)	Air	Insulator (Al)	SCM
	^{12}C		8.374-2						1.185-2			
O	^{16}O							3.383-2	6.630-3	1.17-5		
	^{4}He				1.0-4	1.0-5	1.0 -5					
	Nb											3.884-3
O	Mo			1.255-3		1.130-3	2.134-4		5.020-4			7.530-4
O	Cr			1.575-2		1.418-2	2.678-3		6.300-3			9.450-3
O	Ni			9.848-3		8.863-3	1.674-3		3.939-3			5.909-3
O	Fe			5.909-2		5.318-2	1.005-3	3.176-2	2.364-2			3.545-2
O	H	1.0-11						1.861-2	1.326-2			
O	^{10}B							5.601-5	3.764-2			
	N									4.22-5		
O	Al							2.728-3			1.801-2	
O	Cu											2.370-2
	Ca							2.155-3				
O	^{182}W						1.215-2					
O	^{183}W						6.577-3					
O	^{184}W						1.398-2					
O	^{186}W						1.297-2					
Total Width(cm)		208.5	0.5	6	5	9	24	30	10	10	20	90

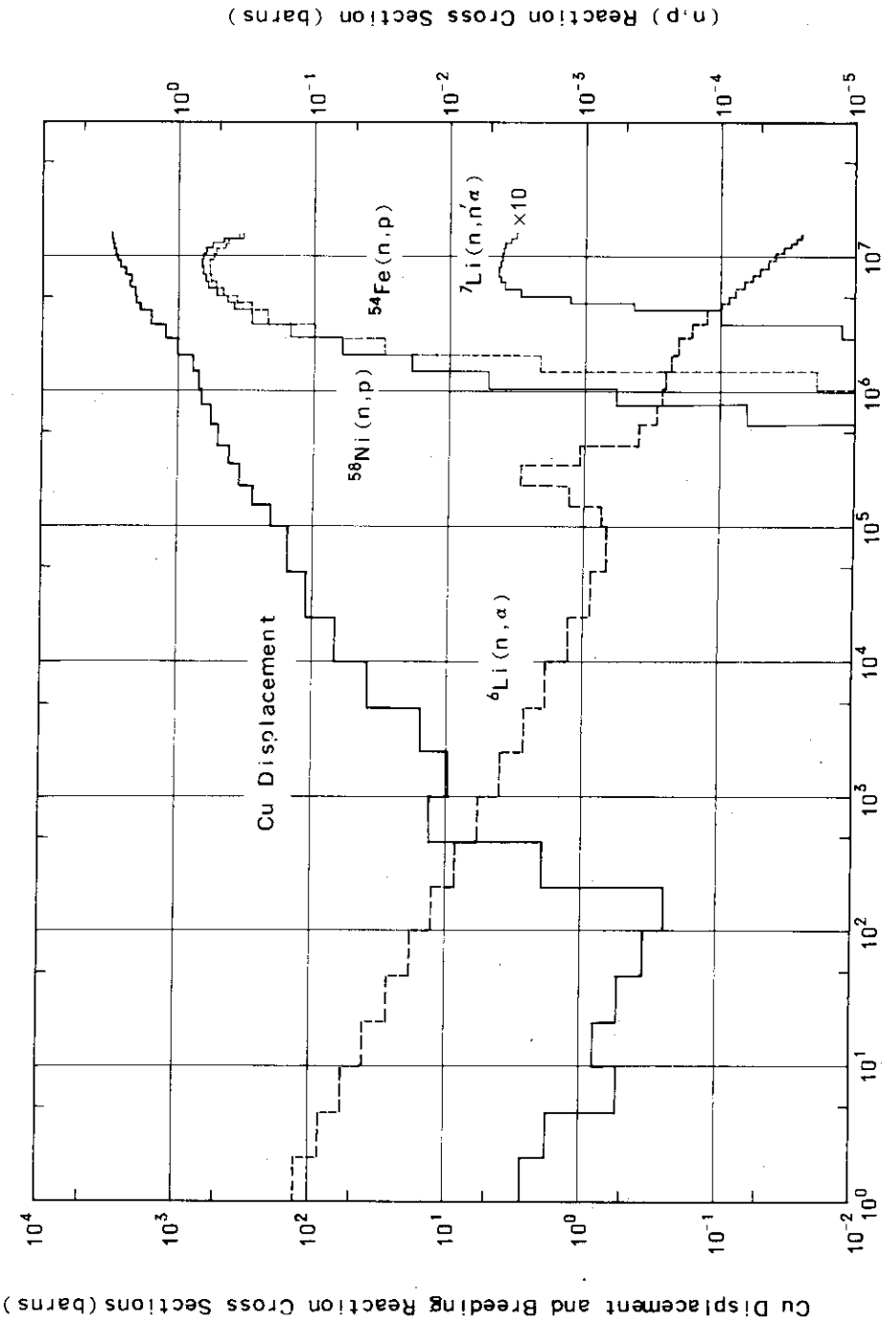

Fig. 2.1 Response Function Profiles Used in Sensitivty Study

3. CALCULATIONAL RESULTS

3.1 Sensitivity of the tritium breeding ratio

Sensitivities of tritium production reaction rates for the total cross sections of the constituent elements of the outer part of JXFR are shown in Table 3.1. Values represent indirect changes of reaction rates when all the cross sections of a constituent element increase by 1%. When a tritium production cross section is increased by a small amount, it corresponds to the increase of the tritium production reaction rates by the equal amount of ratio. This direct effect due to the increase of the tritium production cross section itself is excluded. For example, $^{7}Li(n,n'\alpha)T$ reaction rate in the pebble region decreases by 0.024%, when all types of ^{7}Li cross sections except the tritium production cross section increase by 1%. But when the direct effect is taken into account, the reaction rate increases by 0.976%.

Sensitivity profiles of tritium production reaction ratis in Li_2O pebble and block regions are shown in Figs. 3.1 ∿ 3.16. The ordinate represents the sensitivity per unit lethargy. Solid lines of profiles denote negative sensitivities, while dotted lines positive.

In case of sensitivities of the $^{6}Li(n,\alpha)$ reaction rate in the pebble region, most of the sensitivities for elements except ^{6}Li are positive as shown in Table 3.1. The reason is as follows. The value of the $^{6}Li(n,\alpha)$ reaction cross section becomes larger as the energy of neutron decreases as can be seen in Fig. 2.1. Therefore the more neutrons are moderated, the more $^{6}Li(n,\alpha)$ reactions take place. As a result, the increase of total cross sections of elements except ^{6}Li results in neutron slowing down rather than absorption, and increases $^{6}Li(n,\alpha)$ reactions. As for ^{6}Li, the total cross section is mostly comprised of the $^{6}Li(n,\alpha)$ cross section. Therefore the $^{6}Li(n,\alpha)$ reaction rate decreases by the increase of the ^{6}Li total cross section, when the direct increase of the response is not taken into account. Sensitivity profiles of the $^{6}Li(n,\alpha)$ reaction rate in the pebble region are shown in the odd numbered figures from Fig. 3.1 to Fig. 3.15. The sensitivity profile for ^{6}Li total cross section is negative at all energy except at around 10 MeV. The profiles for other elements are mostly positive. These are consistent with the above discussions. As it is shown in Table 3.1, the negative sensitivity for the total cross section of the ^{6}Li is very large, and almost cancels out the sum of the positive sensitivities for ^{7}Li, ^{16}O and Fe. Sensitivities for the other elements are negligibly small compared with those for the above

four elements.

As for the sensitivities of the $^{7}Li(n,n'\alpha)$ reaction rate in the Li_2O pebble region, negative sensitivities can be seen for the total cross sections of all elements except for those of some elements in the Li_2O block region in Table 3.1. Sensitivities for the total cross sections of ^{12}C, ^{6}Li, ^{7}Li and ^{16}O are very small as the cross sections of these elements are small above the threshold energy of the $^{7}Li(n,n'\alpha)$ reaction. On the other hand, sensitivities for the total cross sections of Cr, Fe and Ni which comprise stainless steel are negative and fairly large, since these elements have comparatively large inelastic cross sections. The sensitivity for Fe is the largest, and the sensitivities for the other elements are nearly less than a quarter of that for Fe. The sensitivity profiles of the $^{7}Li(n,n'\alpha)$ reaction rate in Li_2O pebble region are shown in the odd numbered figures from Fig. 3.1 to Fig. 3.15 together with those of the $^{6}Li(n,\alpha)$ reaction rate. All of them have negative values at almost every energy, because the increase of the total cross section causes the decrease of high energy neutrons.

Sensitivities of the $^{6}Li(n,\alpha)$ reaction rate in Li_2O block region are small for most of elements but ^{6}Li compared with those in Li_2O pebble region. Besides they are mostly negative. This is caused by the negative sensitivity due to the increase of absorption of slow neutrons which cancels out the positive sensitivity by the increase of fast neutron slowing down. The sensitivity to the ^{6}Li is the only exception which takes a very large negative value, because the total cross section of ^{6}Li is mostly comprised of the $^{6}Li(n,\alpha)$ cross section. Sensitivities to the other elements are less than one tenth that for ^{6}Li, and almost negligible. Sensitivity profiles are shown in the even numbered figures from Fig. 3.2 to Fig. 3.16. Those take mostly negative value.

Sensitivities of the $^{7}Li(n,n'\alpha)$ reaction rates in the Li_2O block region have the similar tendency to those of the $^{7}Li(n,n'\alpha)$ reaction rates in the Li_2O pebble region. In this case, all sensitivities are negative owing to the high threshold of the $^{7}Li(n,n'\alpha)$ reaction. The largest value is for Fe, the second is for ^{7}Li and the third is for ^{16}O. Sensitivities for the other elements are even smaller. Sensitivity profiles are shown in even numbered figures from Fig. 3.2 to Fig. 3.16. All values of the profiles are negative.

Sensitivities of tritium production reaction rates are summarized in Table 3.2. The upper half summarizes the sensitivities for the total cross section of elements in all regions. And absolute values of the

tritium production reaction rate changes due to the increase of total cross sections of elements are shown below them. In the second lowest columm, the absolute reaction rates are summed up. The largest change of the tritium breeding ratio is 0.753 due to the 1 percent increase of total cross section for the ^{6}Li. The second and the third largest is the decrease for the Fe and the ^{16}O, which is only some one tenth compared with the change due to the increase for the ^{6}Li. Changes for the other elements are much less than one tenth for ^{6}Li. All of changes due to the increase of total cross sections are negative. Sensitivities of the tritium production reaction rate in all Li_2O regions are shown in the lowest column of Table 3.2.

3.2 Sensitivity of the activation reaction rate in the outer part of the superconducting magnet

Sensitivities of $^{58}Ni(n,p)$ and $^{56}Fe(n,p)$ reaction rates in the outer part of the superconducting magnet for the total cross sections of the constituent elements of the outer part of JXFR are shown in Tables 3.3 and 3.4. The values for Ni and Fe exclude the direct change of the reaction rates due to the change of the (n,p) reaction cross sections themselves.

Sensitivities of both (n,p) reaction rates are negative at every energy for total cross sections of elements in all regions. This is because the neutrons with energy above the (n,p) reaction threshold in the superconducting magnet always decrease, when total cross sections of elements increase. The sensitivity for Fe total cross section is found to be the largest among the sensitivities of $^{58}Ni(n,p)$ reaction rate integrated throughout regions shown in Table 3.3. When the total cross section of Fe is increased by 1 per cent, $^{58}Ni(n,p)$ reaction rate decreases by 8.5 percent. The second largest is that for ^{16}O cross section, and the sensitivity is nearly half the value for Fe. Sensitivities for the cross section of the other elements are less than a quarter of the sensitivity for Fe. Judging from the values in Table 3.3, Li_2O block, stainless steel block and heavy concrete with borated water play an important role in shielding superconducting magnet.

As for the sensitivities of the $^{56}Fe(n,p)$ reaction rate given in Table 3.4, similar tendencies as for the $^{58}Ni(n,p)$ reaction rate can be seen except that values become a little larger. Similarity of the tendencies comes from the similarity of both cross sections as shown in Fig. 2.1. A little

higher threshold energy of $^{56}Fe(n,p)$ reaction results in a little larger sensitivities.

Sensitivity profiles of the two (n,p) reaction rates are shown in Figs.3.17 and 3.18. In order to help us compare a sensitivity profile with another one, those which show similar features are plotted over the same energy scale. The sensitivity profile for Fe total cross section is added to each energy scale for comparison. These sensitivity profiles of (n,p) reaction rates are all negative.

Figure 3.17 shows sensitivity profiles of $^{58}Ni(n,p)$ reaction rates. Since there is a strong 14 MeV neutron peaking in Li_2O pebble and block regions, the sensitivities for ^{6}Li and ^{7}Li are especially large near 14 MeV. Sensitivities for Cr, Mo and Ni are similar to that for Fe, because their distribution is similar as they are included as stainless steel components and their cross sections are alike. The sensitivity for ^{16}O is the second largest, the profile of which happens to be very similer to that for Fe in shape and in magnitude. The sensitivity for H is relatively large but lacks the 14 MeV peak. This is because hydrogen exists only in a region far from the plasma.

Figure 3.18 shows the sensitivity prefiles of $^{56}Fe(n,p)$ reaction rates. Many features of the profiles are quite similar to those of $^{58}Ni(n,p)$ reaction rates as is expected from the similarity of the (n,p) reaction cross sections.

3.3 Sensitivity of atomic displacement rate of Cu stabilizer in the inner part of the superconducting magnet

The sensitivity of atomic displacement rate of Cu stabilizer in the inner part of the superconducting magnet for total cross sections of constituent elements which compose inner part of JXFR is shown in Table 3.5.

Sensitivity for the total cross section of Fe is the largest among the 13 elements which were studied. Because Fe is the principal elements of the stainless steel, which is the structural material of the inner blanket as well as the shield region. The displacement rate decreases by 4.2% due to the increase of 1% total cross section of Fe. Second notable are the sensitivities for isotopic elements of tungsten which are contained in the inner blanket to improve its ability to shield. Sensitivity for the total cross section of each tungsten isotope is from 14% to 30% that for Fe. The total sensitivity for all isotopes of tungsten is almost equal to that for Fe even though the

effective thickness of tungsten is much smaller than that of iron. This demonstrates the effectiveness of tungsten as a shield material of the inner blanket. The sensitivity for ^{16}O which is included as water coolant of the shield region is also notable with about 30% the value for Fe.

Figures 3.19 and 3.20 show the sensitivity profiles of Cu atomic displacement rate for the total cross sections of constituent element of inner part of JXFR. All sensitivity values of profiles are negative even though those for Fe are denoted by dashed lines. Cr and ^{184}W are constituent elements of the inner blanket where the neutron spectrum is very hard. Hence the sensitivity profiles for Cr and ^{184}W are very high in the high energy region. On the contrary, H and ^{10}B are only in the shield region and profiles for them are fairly high even in low energy region around 1 MeV.

Table 3.1 Sensitivity of Tritium Production Reaction Rates in Li_2O Pebble and Block Regions for the Total Cross Sections of JXFR Constituent Elements

Reaction*) (Rate)	Reg. No.	Region	Sensitivity for Elements							
			^{12}C	^{6}Li	^{7}Li	^{16}O	Cr	Fe	Ni	Mo
T_6(Pebble) (0.207)	3	Carbon coating	0.029							
	4	Stainless Steel					0.015	0.070	-0.002	-0.001
	5	Li_2O Pebble		-0.430	0.149	0.106	0.026	0.104	0.009	-0.001
	6	Li_2O Block		-0.294	0.100	0.099	0.019	0.078	0.016	0.002
	Total		0.029	-0.725	0.249	0.204	0.060	0.253	0.024	0.0
T_7(Pebble) (0.117)	3	Carbon coating	-0.035							
	4	Stainless Steel					-0.045	-0.158	-0.027	-0.003
	5	Li_2O Pebble		-0.005	-0.037	-0.067	-0.039	-0.136	-0.024	-0.002
	6	Li_2O Block		0.0	0.014	0.004	-0.003	-0.009	-0.002	0.0
	Total		-0.035	-0.005	-0.024	-0.063	-0.087	-0.304	-0.052	-0.005
T_6(Block) (0.627)	3	Carbon coating	-0.029							
	4	Stainless Steel					-0.004	0.008	-0.010	0.002
	5	Li_2O Pebble		-0.155	-0.037	-0.064	-0.008	-0.007	-0.015	0.0
	6	Li_2O Block		-0.796	0.043	-0.010	-0.007	-0.016	-0.013	-0.004
	7	S.S. Block					0.001	0.005	0.002	-0.002
	8	Stainless Steel					0.0	0.001	0.0	0.0
	Total		-0.029	-0.951	0.006	-0.074	-0.017	-0.009	-0.035	-0.004
T_7(Block) (0.139)	3	Carbon coating	-0.035							
	4	Stainless Steel					-0.036	-0.129	-0.022	-0.003
	5	Li_2 Pebble		-0.016	-0.197	-0.170	-0.060	-0.217	-0.037	-0.005
	6	Li_2 Block		-0.027	-0.296	-0.234	-0.064	-0.234	-0.041	-0.005
	Total		-0.035	-0.043	-0.493	-0.404	-0.160	-0.580	-0.100	-0.013

Sensitivity values less than 10^{-3} are assigned 0.0 or omitted from the table.

*) T_6(Pebble) denotes $^{6}Li(n,\alpha)t$ reaction in the Li_2O pebble region, and T_7(Pebble) denotes $^{7}Li(n,n'\alpha)t$ reaction in the same region.

Table 3.2 Summary of the Sensitivities of Tritium Production Reaction Rates

Contents	Reaction*) (Rate)	Total Sensitivity or Reaction Rate Change for Elements							
		^{12}C	^{6}Li	^{7}Li	^{16}O	Cr	Fe	Ni	Mo
Total Sensitivity for Elements	T_6(Pebble)	0.029	-0.725	0.249	0.204	0.060	0.253	0.024	0.0
	T_7(Pebble)	-0.035	-0.005	-0.024	-0.063	-0.087	-0.304	-0.052	-0.005
	T_6(Block)	-0.029	-0.951	0.006	-0.074	-0.017	-0.009	-0.035	-0.004
	T_7(Block)	-0.035	-0.043	-0.493	-0.404	-0.160	-0.580	-0.100	-0.013
Reaction Rate Change for the Increase of Total cross Section by 1%	T_6(Pebble) (0.207)	0.006	-0.150	0.052	0.042	0.012	0.052	0.005	0.0
	T_7(Pebble) (0.117)	-0.004	-0.001	-0.003	-0.007	-0.010	-0.036	-0.006	-0.001
	T_6(Block) (0.627)	-0.018	-0.596	0.004	-0.046	-0.011	-0.006	-0.022	-0.003
	T_7(Block) (0.139)	-0.005	-0.006	-0.068	-0.056	-0.022	-0.081	-0.014	-0.002
Total R.R. Change		-0.021	-0.753	-0.015	-0.067	-0.031	-0.071	-0.037	-0.006
Sensitivity of R.R. in All Li_2O Regions		-0.019	-0.691	-0.014	-0.061	-0.028	-0.065	-0.034	-0.006

*) Same difinition as in Table 3.1 is applied.

Table 3.3 Sensitivity of $^{58}Ni(n,p)$ Reaction Rate in the Outer Part of SCM*) for the Total Cross Sections of JXFR Outer Constituent Elements

Zone	Reg. No.	Region	Sensitivity for Elements							
			^{6}Li	^{7}Li	^{16}O	Fe	Cr	Ni	Mo	H
Blanket	4	Stainless Steel				-0.115	-0.032	-0.020	-0.003	
	5	Li_2O Pebble	-0.020	-0.270	-0.188	-0.197	-0.053	-0.034	-0.005	
	6	Li_2O Block	-0.130	-1.748	-1.156	-0.770	-0.203	-0.132	-0.022	
	7	S.S. Block				-2.017	-0.532	-0.350	-0.057	
	8	Stainless Steel				-0.499	-0.132	-0.087	-0.014	
Shield	10	Heavy Concrete + Borated Water			-2.619	-4.474				-1.008
TFC	14	SCM*)				-0.413	-0.121	-0.073	-0.011	
Total			-0.150	-2.018	-3.963	-8.485	-1.073	-0.695	-0.113	-1.008

*) SCM : Superconducting Magnet

Table 3.4 Sensitivity of $^{56}Fe(n,p)$ Reaction Rate in the Outer Part of SCM*) for the Total Cross Sections of JXFR Outer Constituent Elements

Zone	Reg. No.	Region	Sensitivity for Elements							
			^{6}Li	^{7}Li	^{16}O	Fe	Cr	Ni	Mo	H
Blanket	4	Stainless Steel				-0.141	-0.039	-0.025	-0.004	
	5	Li_2O Pebble	-0.024	-0.328	-0.228	-0.240	-0.065	-0.041	-0.007	
	6	Li_2O Block	-0.157	-2.114	-1.400	-0.933	-0.246	-0.160	-0.026	
	7	S.S. Block				-2.425	-0.640	-0.420	-0.069	
	8	Stainless Steel				-0.598	-0.158	-0.104	-0.017	
Shield	10	Heavy Concrete + Borated Water			-3.101	-5.308				-1.199
TFC	14	SCM*)				-0.487	-0.142	-0.087	-0.012	
Total			-0.182	-2.443	-4.729	-10.131	-1.291	-0.836	-0.135	-1.199

*) SCM : Superconducting Magnet

Table 3.5 Sensitivity of Cu Displacement Rate in the Inner Part of SCM*) for the Total Cross Sections of JXFR Inner Constituent Elements

Zone	Reg. No.	Region	Sensitivity for Elements								
			^{182}W	^{183}W	^{184}W	^{186}W	^{16}O	Fe	Cr	Ni	Mo
Blanket	4	Stainless Steel						-0.127	-0.036	-0.022	-0.003
	6	Stainless Steel						-0.128	-0.035	-0.022	-0.003
	7	S.S. + He						-1.040	-0.280	-0.176	-0.028
	8	S.S. + W + He	-1.120	-0.605	-1.284	-1.160		-0.052	-0.138	-0.087	-0.014
	9	Stainless Steel						-0.501	-0.134	-0.084	-0.013
Total			-1.120	-0.605	-1.284	-1.160					

Zone	Reg. No.	Region	Sensitivity for Elements								
			Cu	Al	^{10}B	H					
Shield	11	H.C. + H_2O(B)		-0.124	-0.002	-0.497	-1.194	-1.962			
	12	S.S. + B_4C + H_2O			-0.476	-0.199	-0.067	-0.408	-0.117	-0.073	-0.010
TFC	14	Insulator (Al)		-0.166							
	15	SCM*)	-0.030					-0.002	-0.004	-0.006	0.001
	16	Insulator (Al)		0.0							
Total			-0.030	-0.290	-0.477	-0.696	-1.261	-4.219	-0.745	-0.471	-0.072

*) SCM : Superconducting Magnet

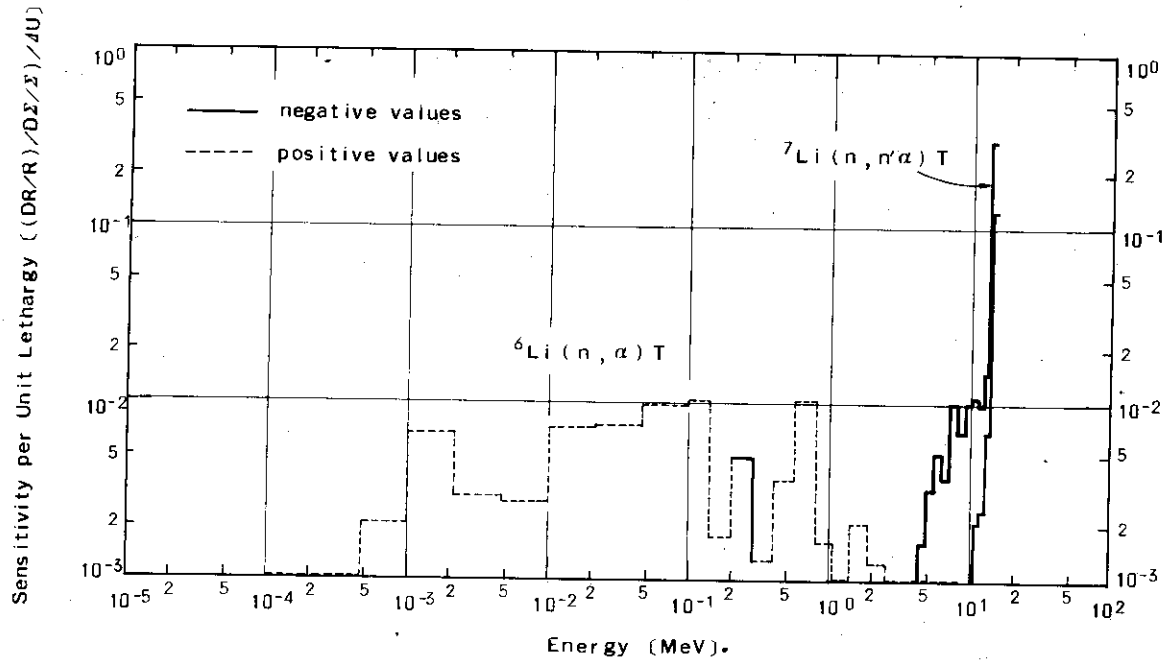

Fig. 3.1 Breeding Ratio Sensitivity per Unit Lethargy versus Energy in Li_2O Pebble Region for ^{12}C Total Cross Section

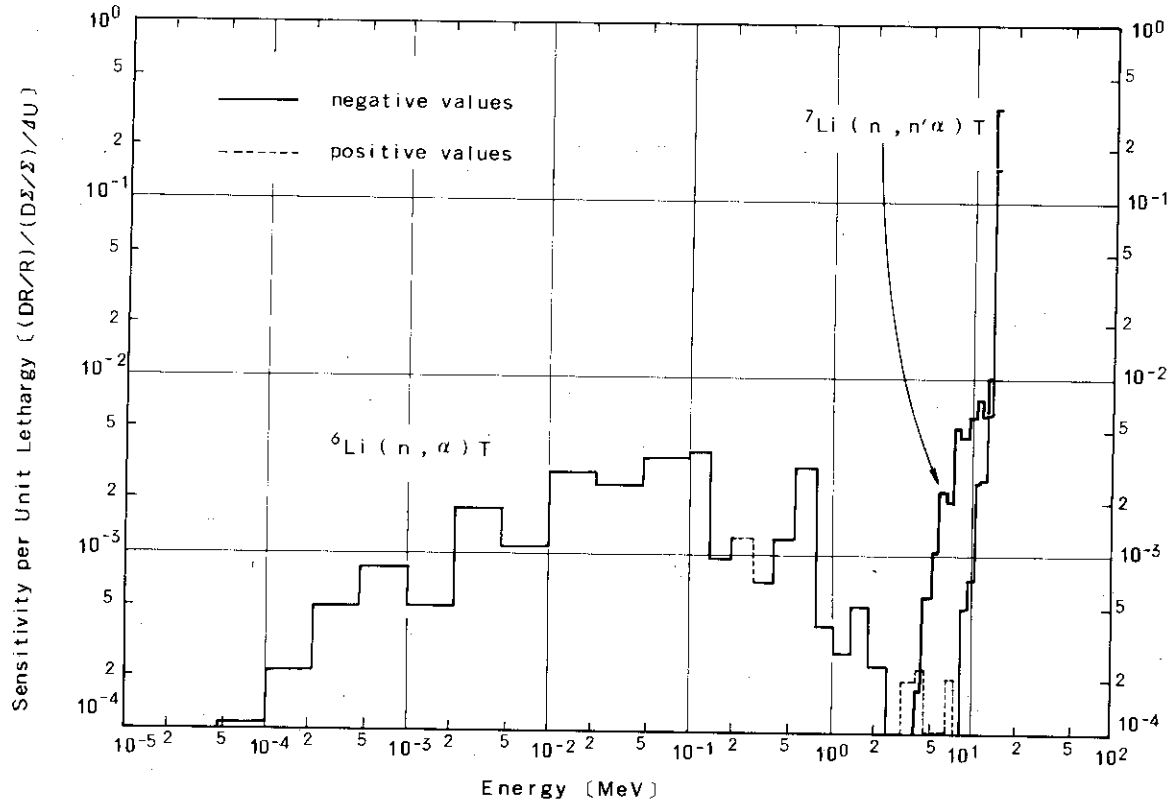

Fig. 3.2 Breeding Ratio Sensitivity per Unit Lethargy versus Energy in Li_2O Block Region for ^{12}C Total Cross Section

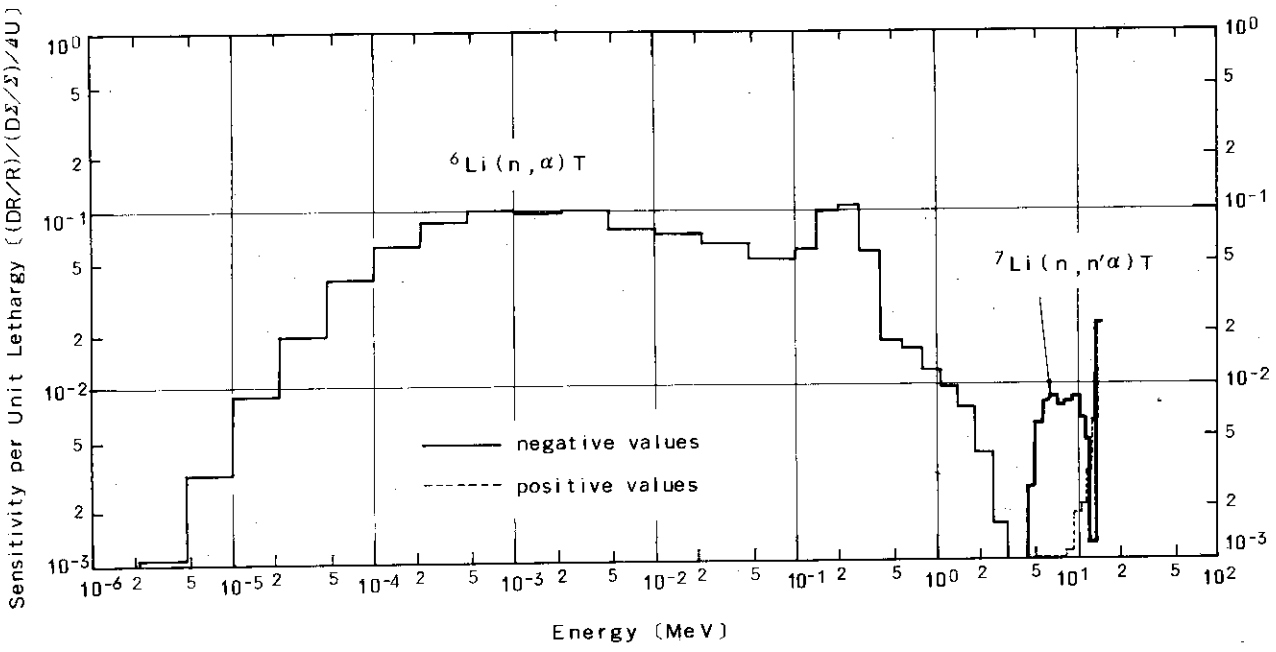

Fig. 3.3 Breeding Ratio Sensitivity per Unit Lethargy versus Energy in Li_2O Pebble Region for ^{6}Li Total Cross Section

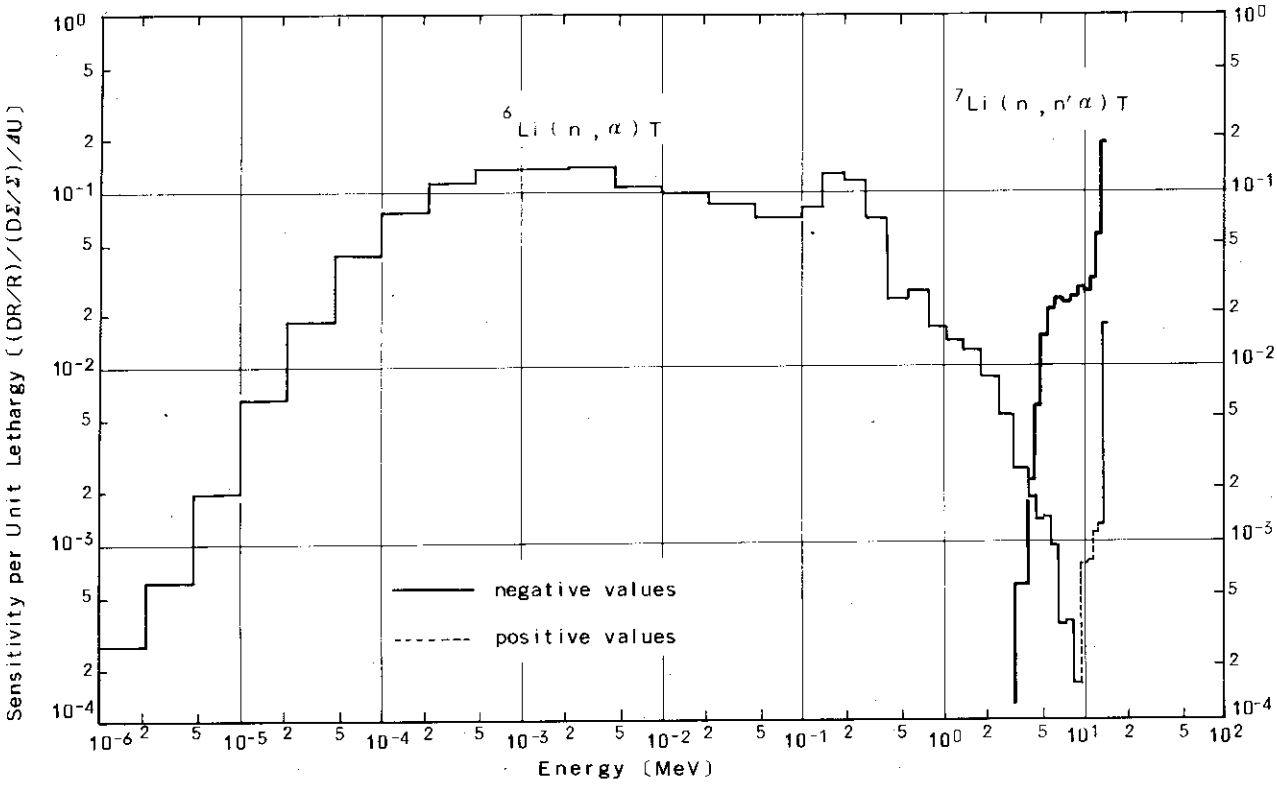

Fig. 3.4 Breeding Ratio Sensitivity per Unit Lethargy versus Energy in Li_2O Block Region for ^{6}Li Total Cross Section

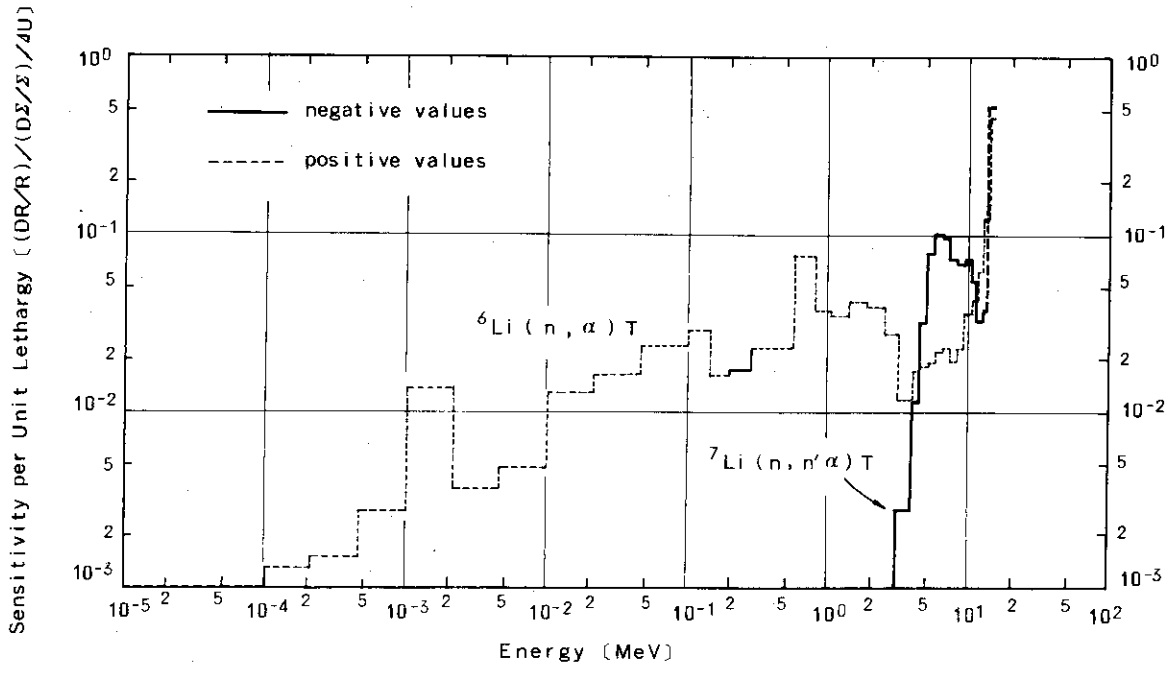

Fig. 3.5 Breeding Ratio Sensitivity per Unit Lethargy versus Energy in Li_2O Pebble Region for ^{7}Li Total Cross Section

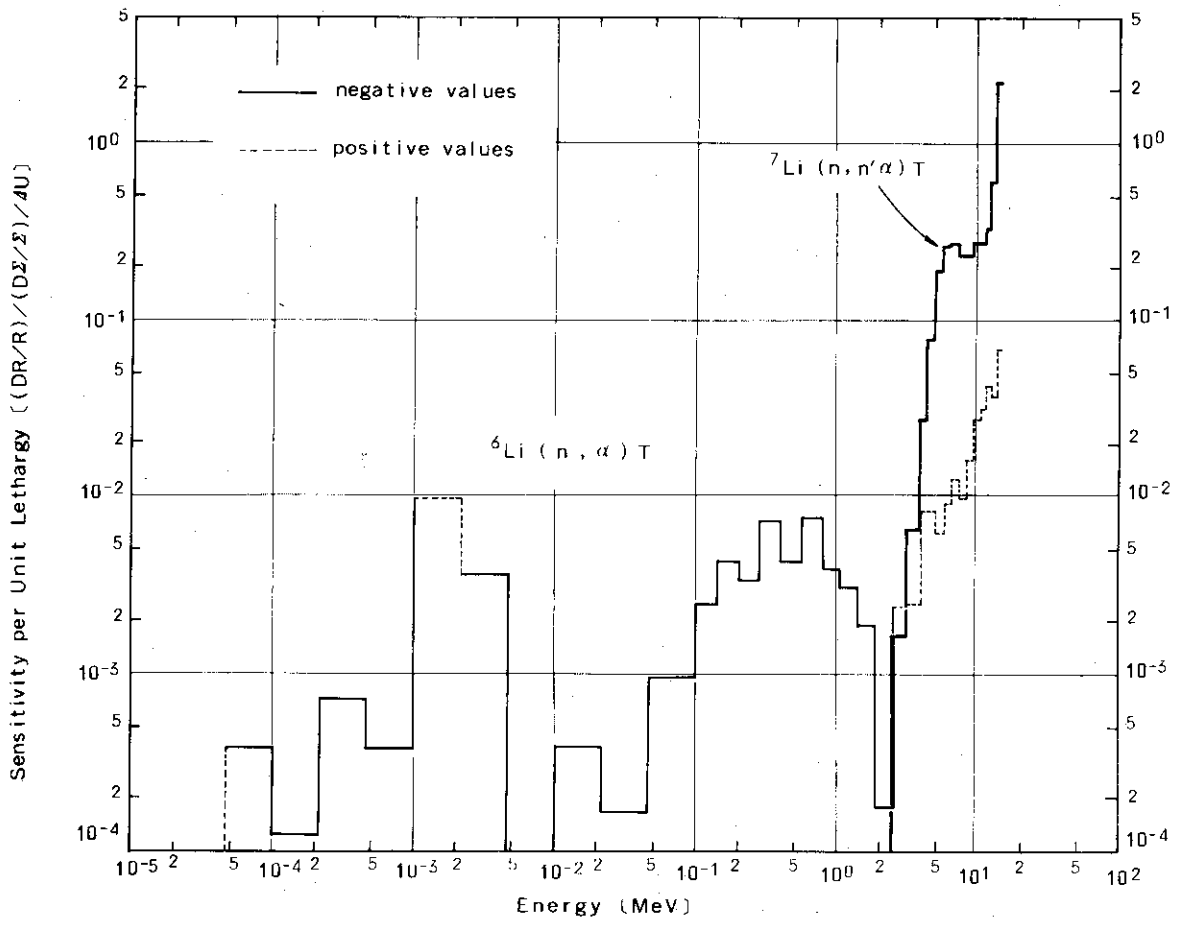

Fig. 3.6 Breeding Ratio Sensitivity per Unit Lethargy versus Energy in Li_2O Block Region for ^{7}Li Total Cross Section

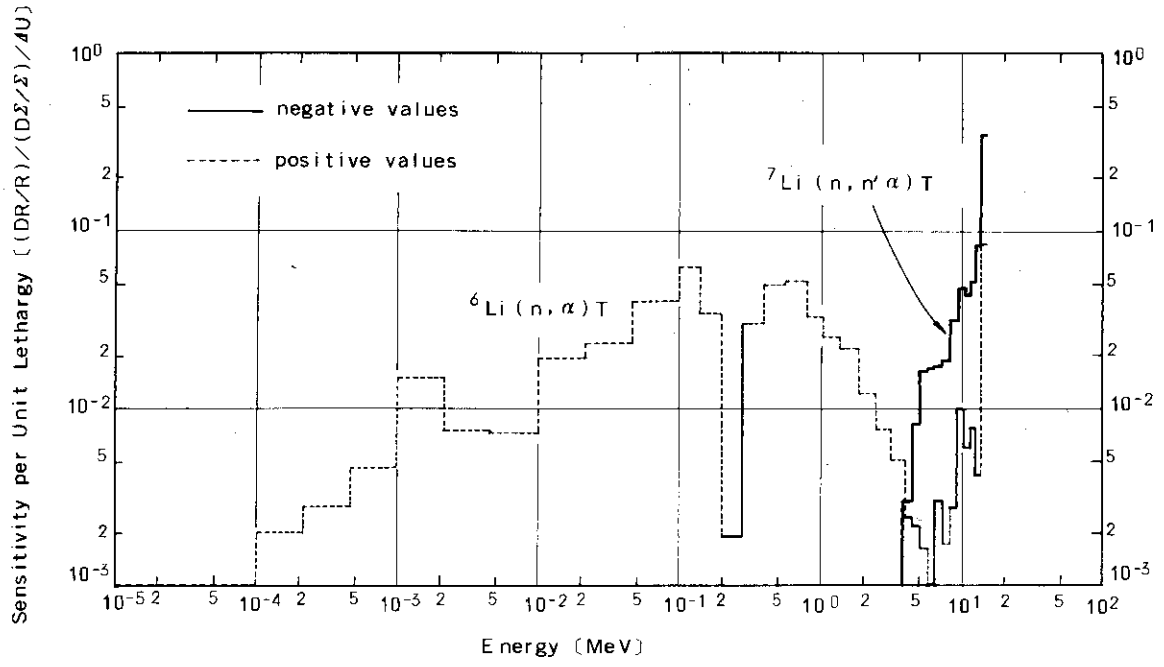

Fig. 3.7 Breeding Ratio Sensitivity per Unit Lethargy versus Energy in Li_2O Pebble Region for ^{16}O Total Cross Section

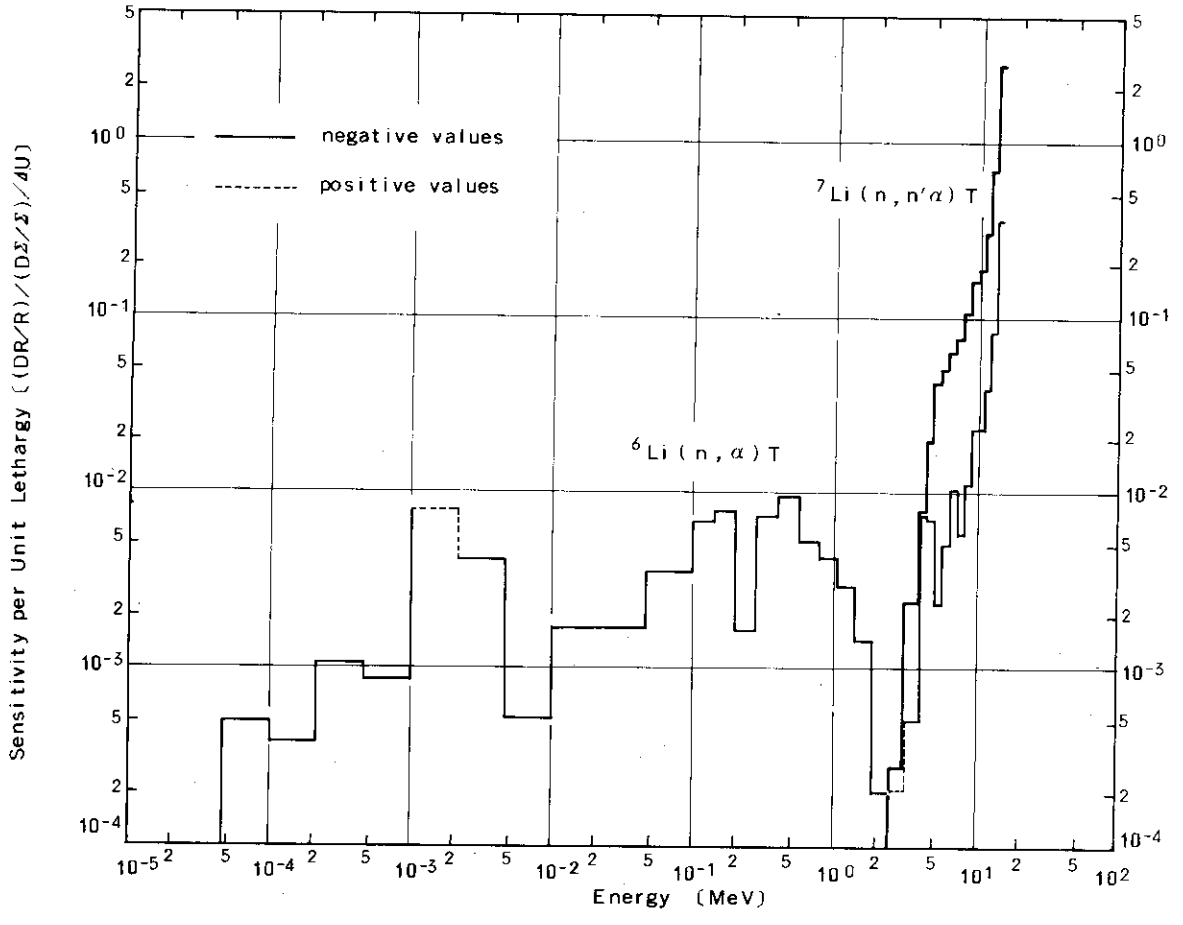

Fig. 3.8 Breeding Ratio Sensitivity per Unit Lethargy versus Energy in Li_2O Block Region for ^{16}O Total Cross Section

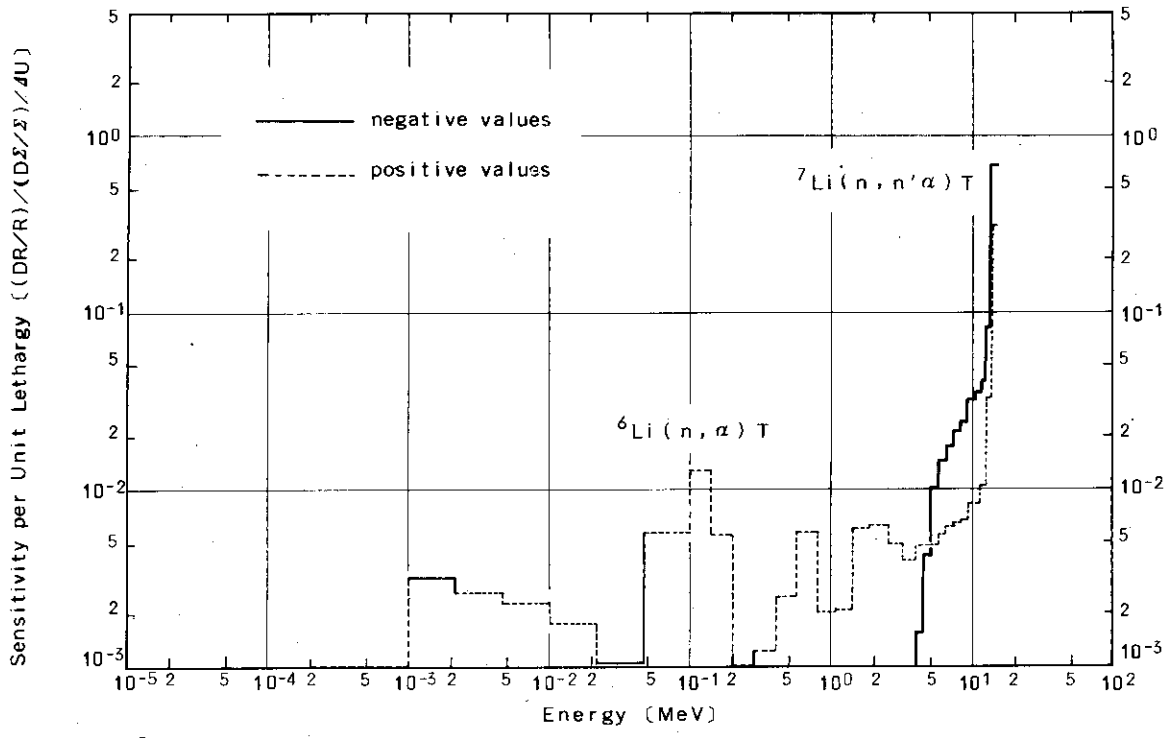

Fig. 3.9 Breeding Ratio Sensitivity per Unit Lethargy versus Energy in Li_2O Pebble Region for Cr Total Cross Section

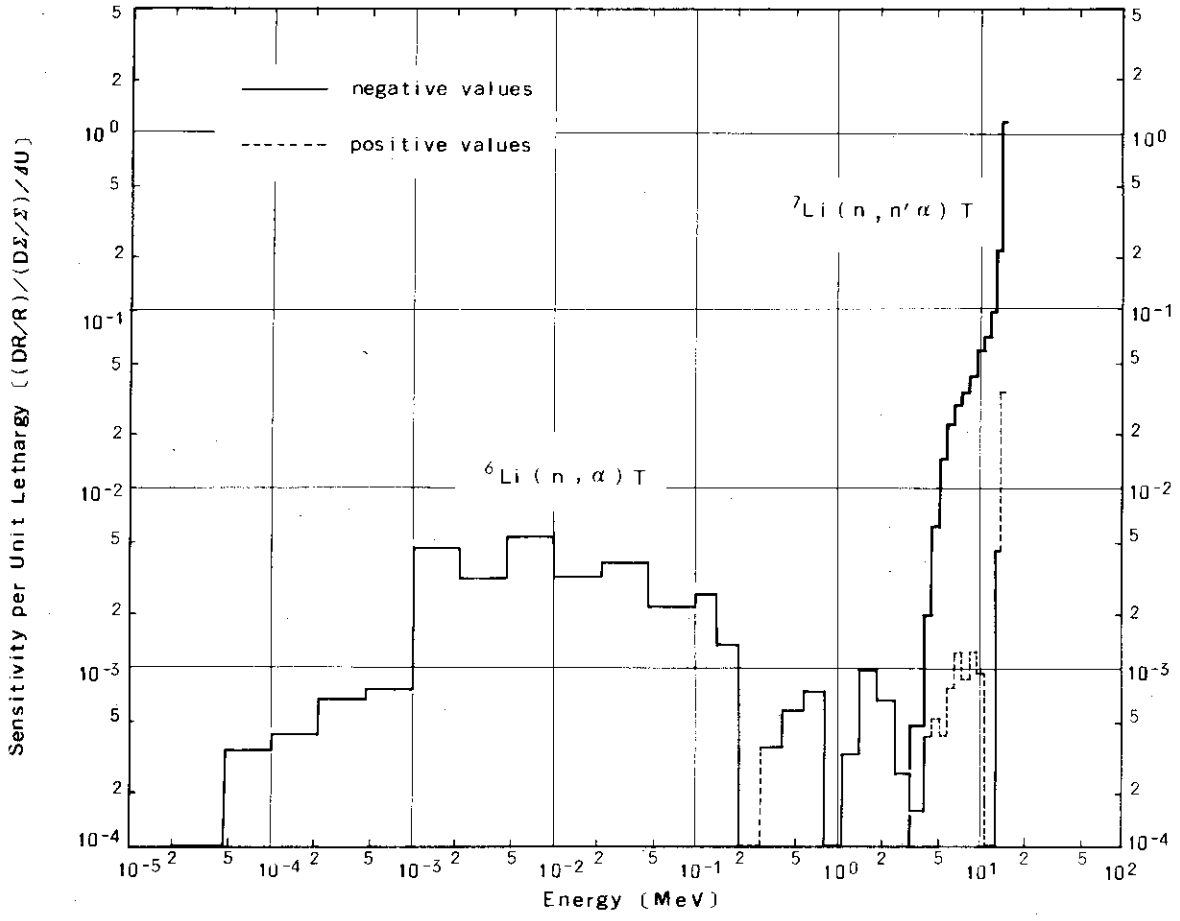

Fig. 3.10 Breeding Ratio Sensitivity per Unit Lethargy versus Energy in Li_2O Block Region for Cr Total Cross Section

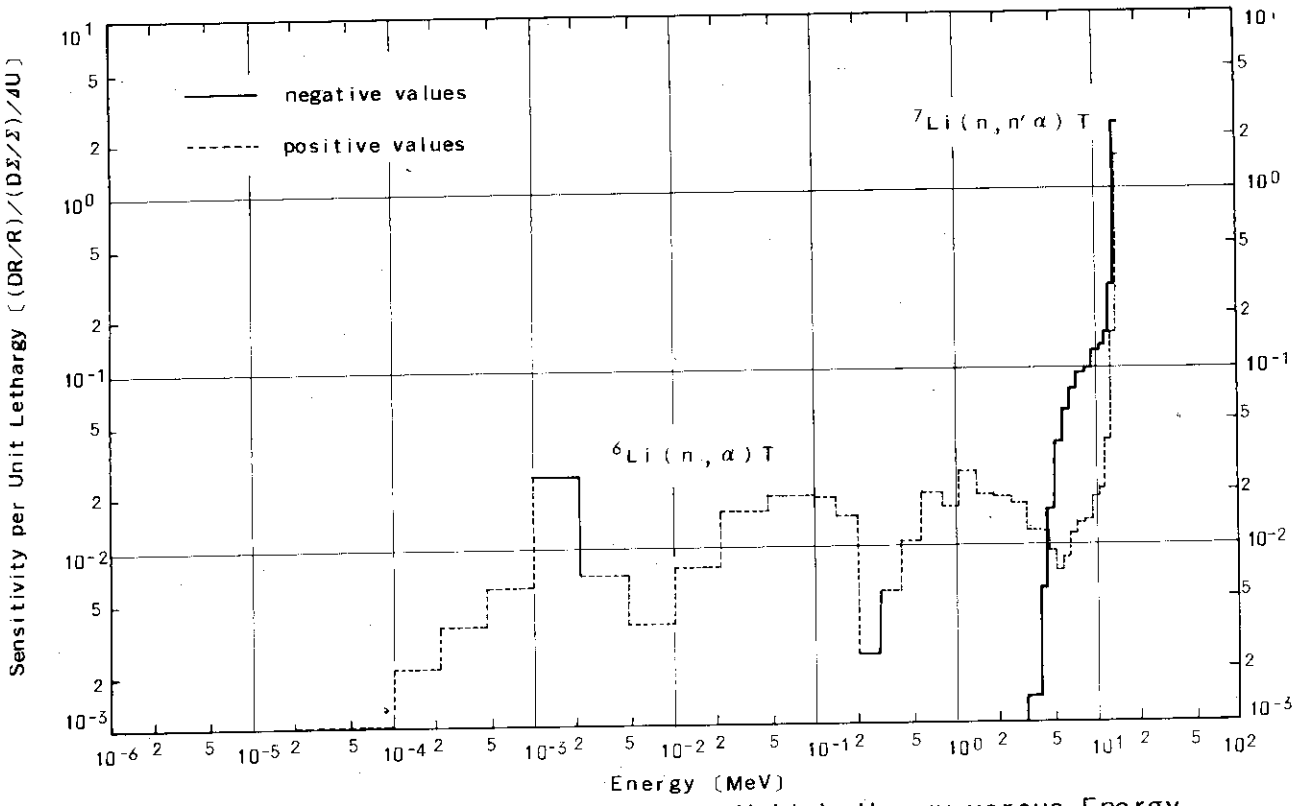

Fig. 3.11 Breeding Ratio Sensitivity per Unit Lethargy versus Energy in Li_2O Pebble Region for Fe Total Cross Section

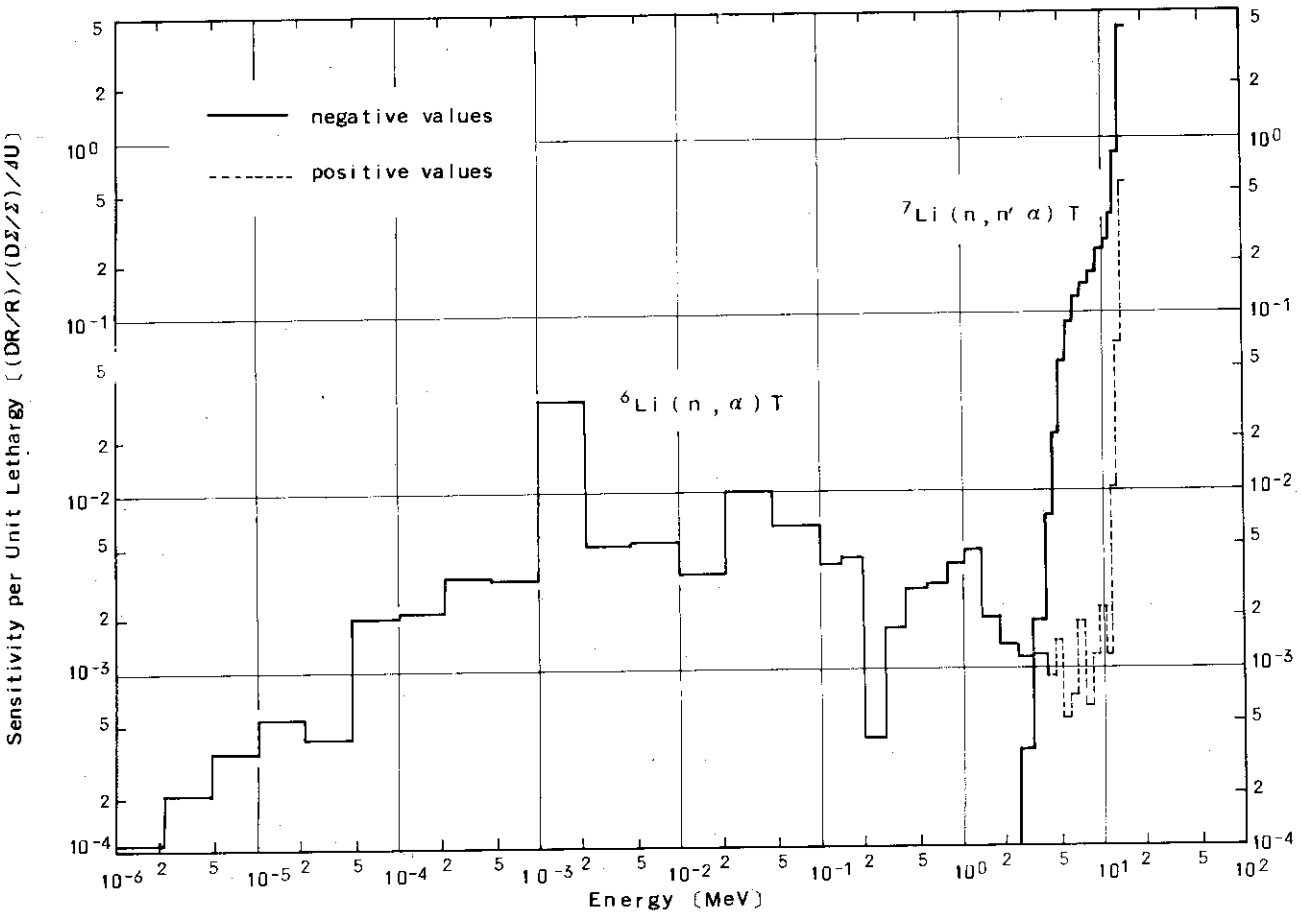

Fig. 3.12 Breeding Ratio Sensitivity per Unit Lethargy versus Energy in Li_2O Block Region for Fe Total Cross Section

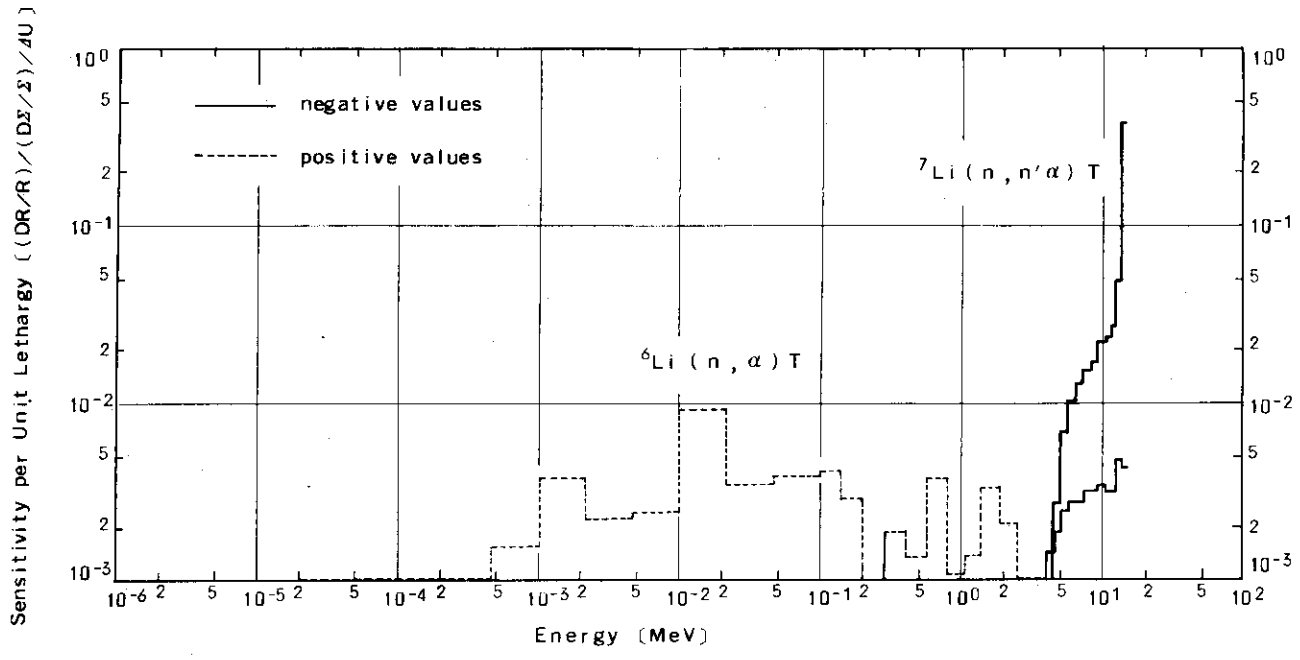

Fig. 3.13 Breeding Ratio Sensitivity per Unit Lethargy versus Energy in Li_2O Pebble Region for Ni Total Cross Section

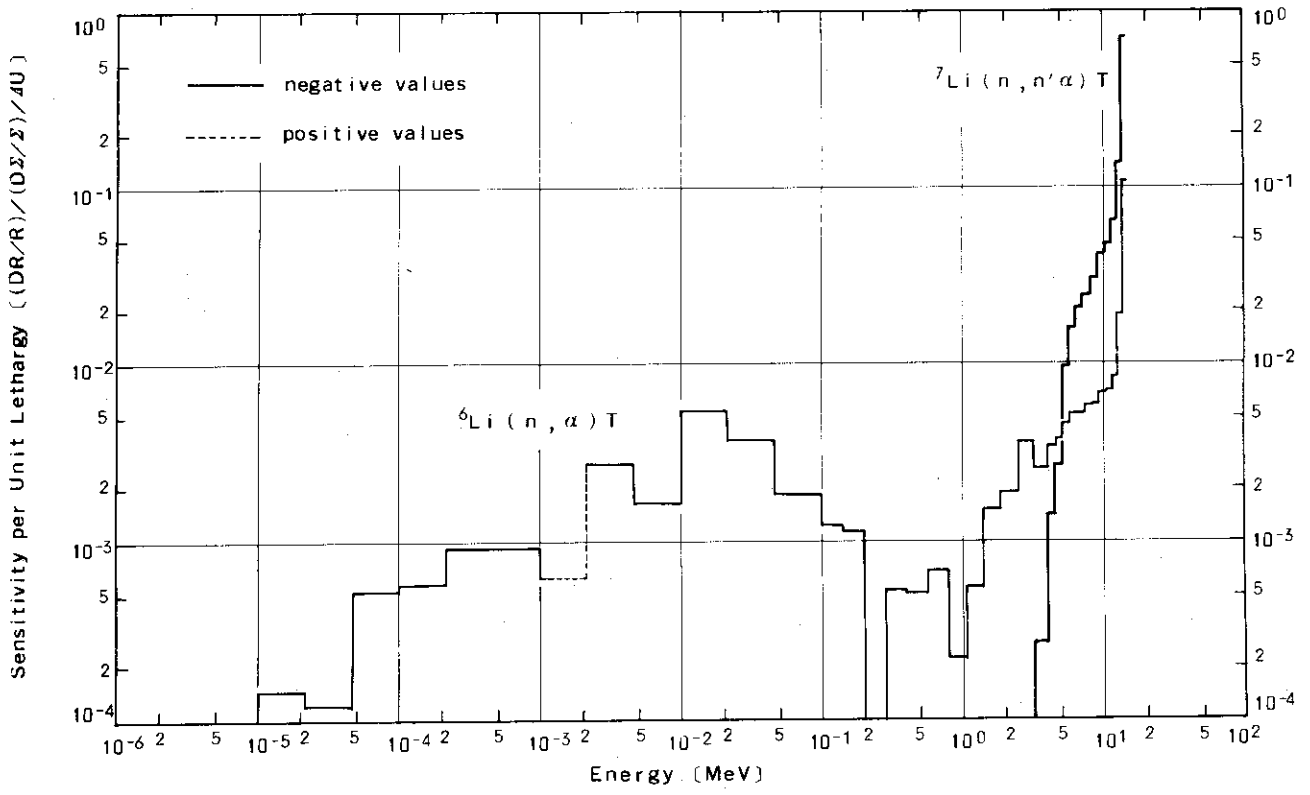

Fig. 3.14 Breeding Ratio Sensitivity per Unit Lethargy versus Energy in Li_2O Block Region for Ni Total Cross Section

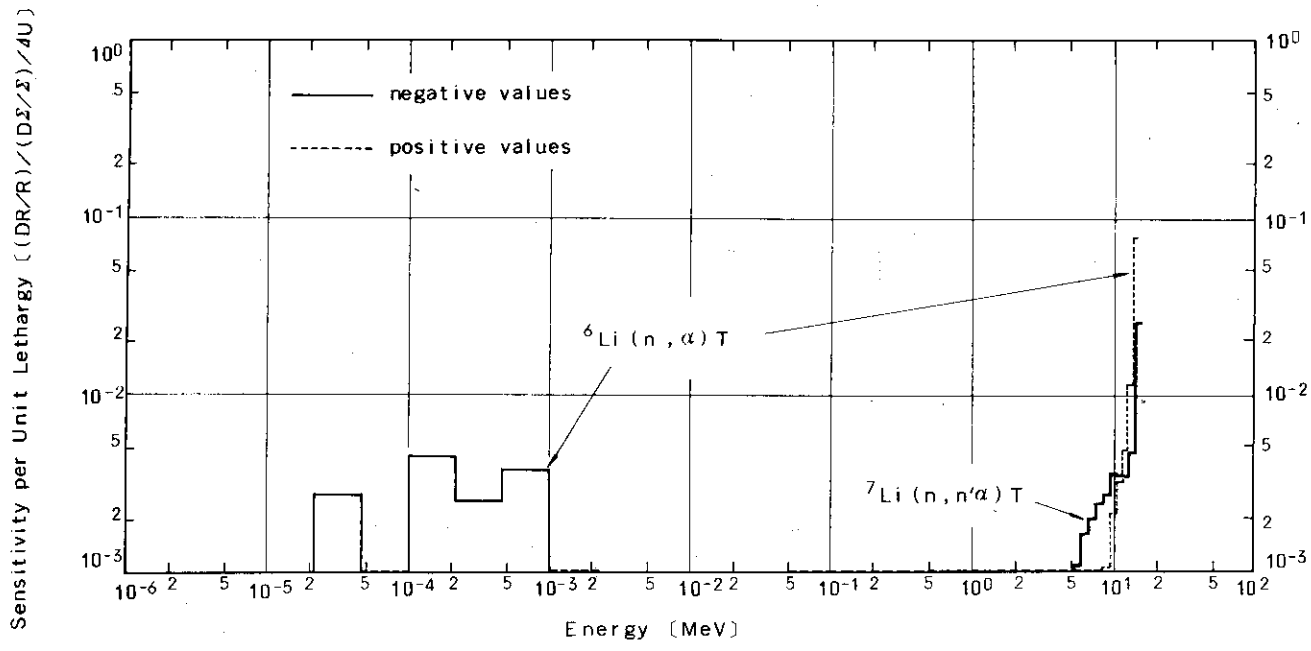

Fig. 3.15 Breeding Ratio Sensitivity per Unit Lethargy versus Energy in Li_2O Pebble Region for Mo Total Cross Section

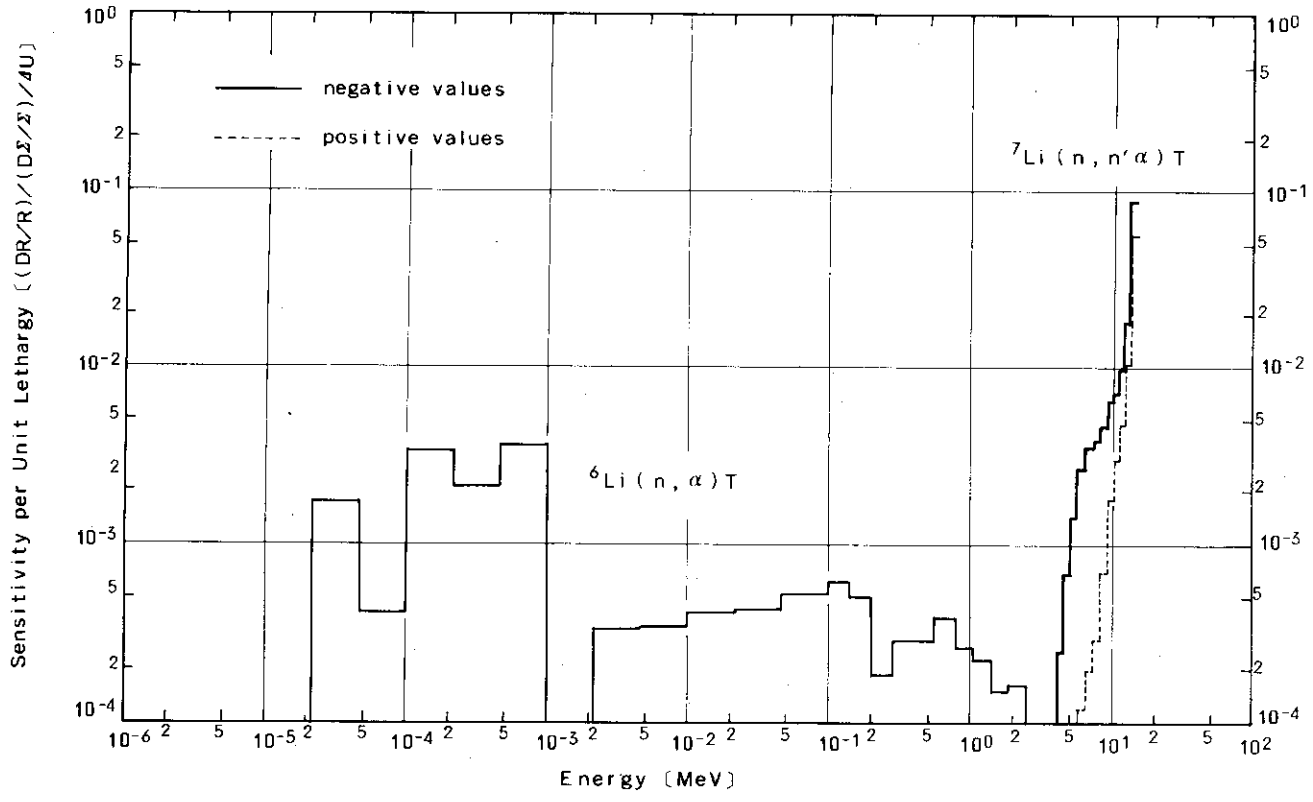

Fig. 3.16 Breeding Ratio Sensitivity per Unit Lethargy versus Energy in Li_2O Block Region for Mo Total Cross Section

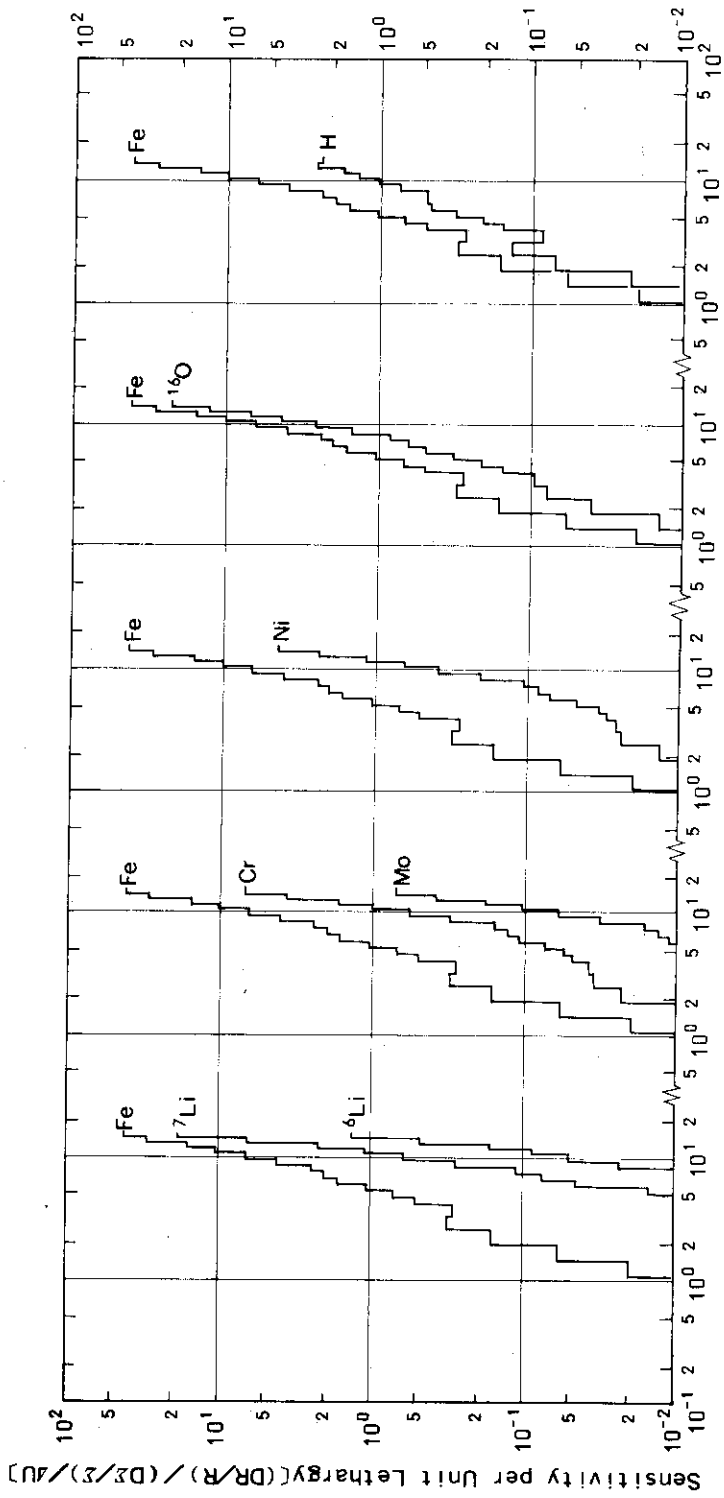

Fig. 3.17 $^{58}Ni(n,p)$ Reaction Sensitivity per Unit Lethargy versus Energy for Constituent Total Cross Sections of JXFR Outer Model

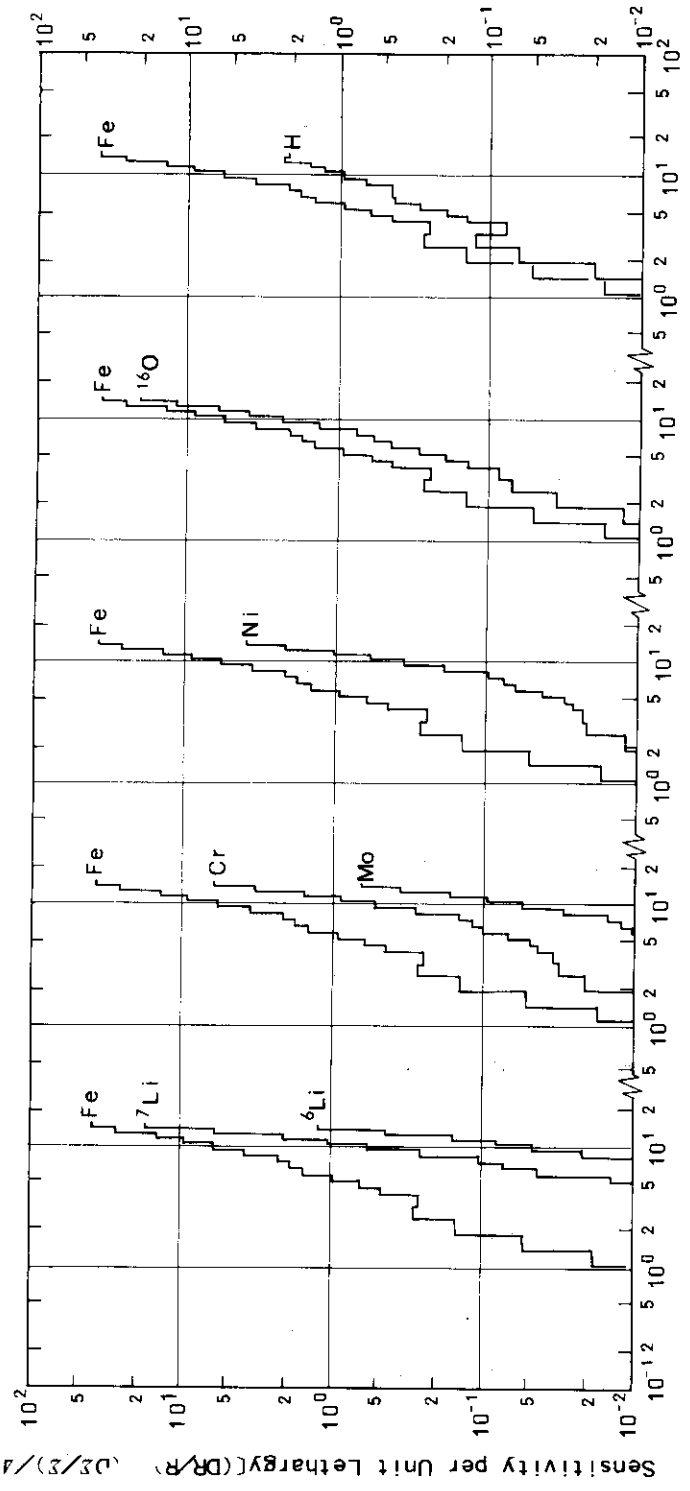

Fig. 3.18 $^{54}Fe(n,p)$ Reaction Sensitivity per Unit Lethargy Versus Energy for Constituent Total Cross Sections of JXFR Outer Model

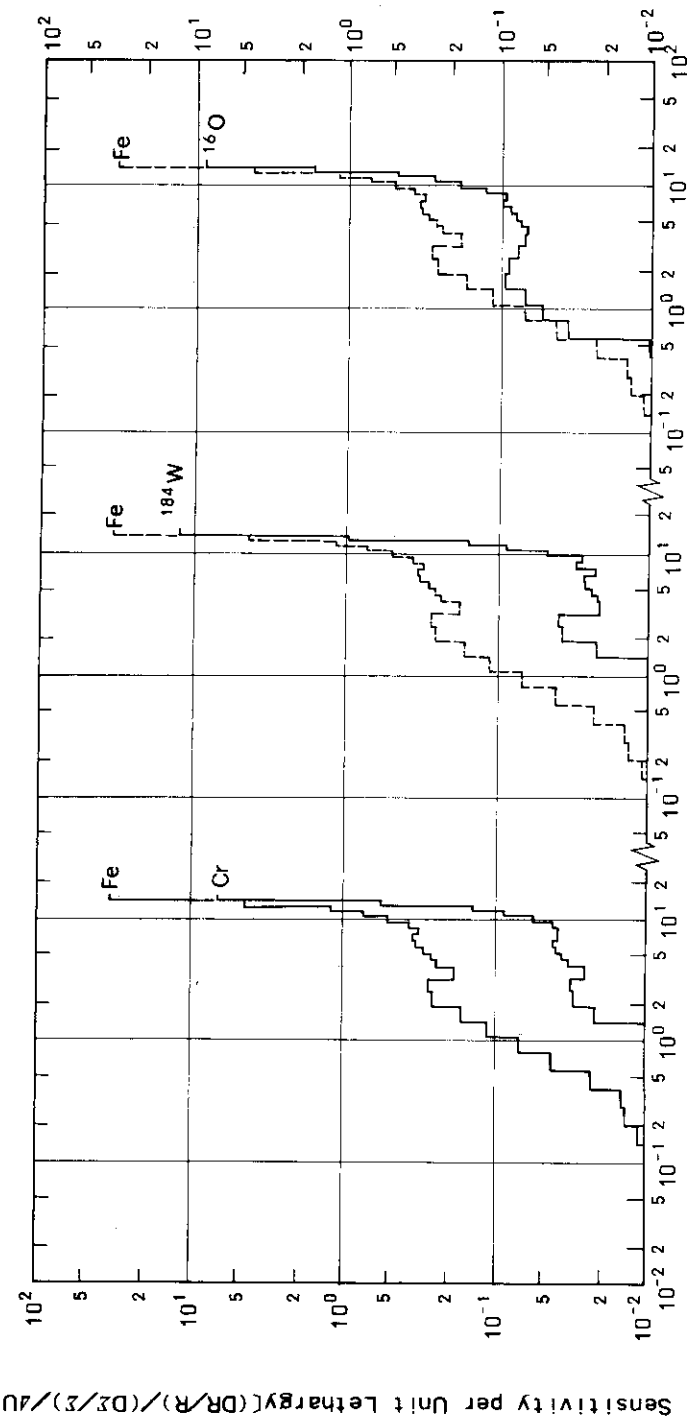

Fig. 3.19 Copper Displacement Sensitivity per Unit Lethargy versus Energy in Inner SCM Region for Fe, Cr, ^{184}W and ^{16}O Total Cross Sections

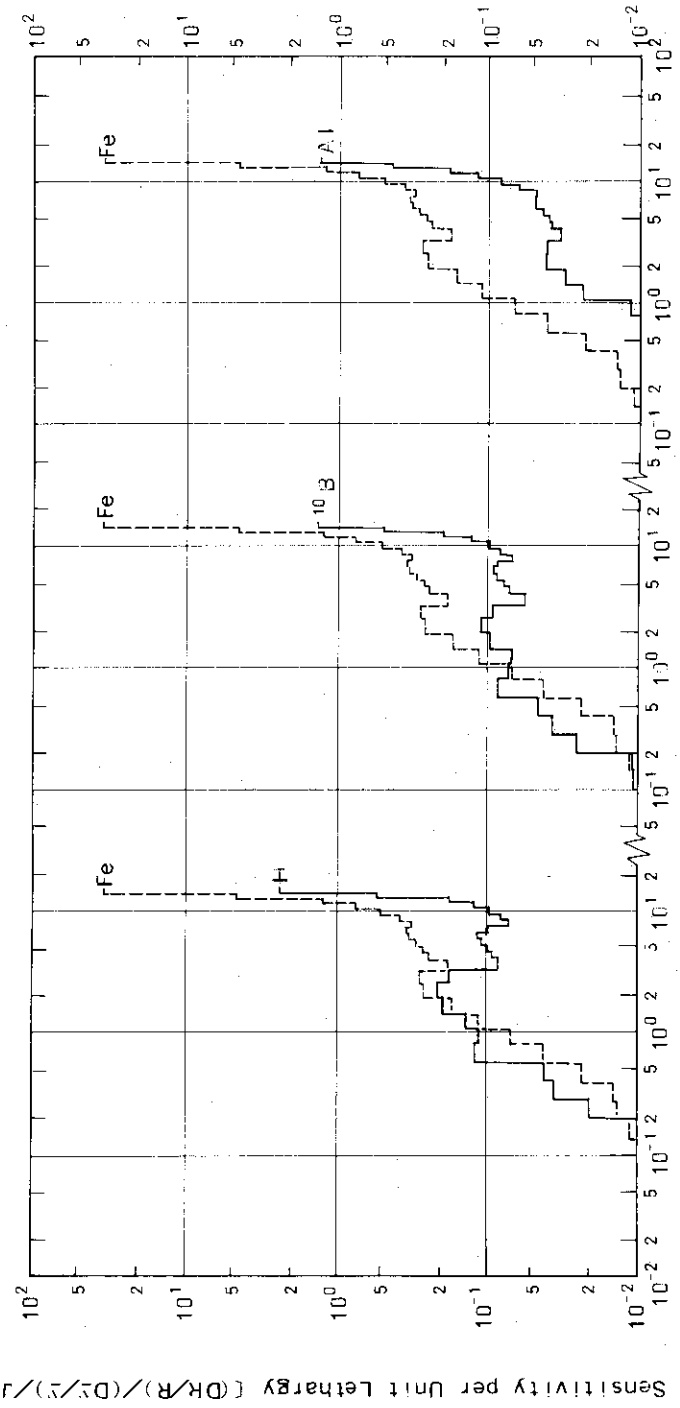

Fig. 3.20 Copper Displacement Sensitivity per Unit Lethargy versus Energy in Inner SCM Region for H, ^{10}B and Al Total Cross Sections

4. DISCUSSIONS

4.1 Sensitivity change due to the difference of the Sn order

In this work, sensitivity study was carried out with $S_{16}P_5$ approximations. And a set of S_8P_5 forward and adjoint calculations were performed to investigate the sensitivity change due to the difference of Sn order. Sensitivities of $^{58}Ni(n,p)$ reaction rate in the outer part of the TFC were calculated using both S_8 and S_{16} appoximations. The comparison of the sensitivities is shown in Table 4.1. The sensitivity change is at most 4.3%, which is very small. The region-wise sensitivity change becomes greater as the region comes nearer to the plasma. For example, the sensitivity change for the total cross section of Fe due to the difference of S_8 and S_{16} is none in the toroidal field coil, and the largest sensitivity change of 4.3% is seen in the innermost stainless steel region. As a result, the sensitivity change due to the difference of S_8 and S_{16} is shown to be caused mainly by the change of adjoint flux rather than forward flux.

4.2 Estimation of reaction rate uncertainty

The results of a sensitivity analysis are utilized in many ways. One of their applications is the error estimation of reaction rate due to the uncertainty of cross section data. In this work, were studied the errors of (n,p) reaction rates in the outer part of the TFC and of copper atomic displacenent rate in the inner part of the coil.

The uncertainty of reaction rate $\Delta R/R$ is described with the sensitivity coefficient P_X^G for the cross section x of energy group G.

$$\left(\frac{\Delta R}{R}\right)^2 = \underset{X,Y,G,G'}{\text{Sum}} P_X^G \cdot P_Y^{G'} \frac{\langle \Delta\Sigma_X^G \cdot \Delta\Sigma_Y^{G'} \rangle}{\Sigma_X^G \cdot \Sigma_Y^{G'}} \qquad (1)$$

where, $\langle \Delta\Sigma_X^G \cdot \Delta\Sigma_{Y'}^{G'} \rangle$ is the covariance matrix element of Σ_X^G and $\Sigma_Y^{G'}$. When a full correlation is supposed, the equation (1) becomes as follows.

$$\left(\frac{\Delta R}{R}\right)^2 = \left(\underset{X,G}{\text{Sum}} P_X^G \cdot \frac{\Delta\Sigma_X^G}{\Sigma_X^G}\right)^2 \qquad (2)$$

And when a no correlation is supposed, the equation (1) becomes as follows.

$$\left(\frac{\Delta R}{R}\right)^2 = \underset{X,G}{\text{Sum}} \left(P_X^G \cdot \frac{\Delta\Sigma_X^G}{\Sigma_X^G}\right)^2 \qquad (3)$$

By the way, as for the energy group, both equations of (2) and (3) involve some defects. That is, the value $\Delta R/R$ might become zero in case of equation (2), and it must be too small and unreasonable in case of equation (3). In order to avoid such inconvenience, the following equation was adopted concerning the summation of the errors over energy groups.

$$\left(\frac{\Delta R}{R}\right)_X = \underset{G}{\text{Sum}} \left| P_X^G \cdot \frac{\Delta\Sigma_X^G}{\Sigma_X^G} \right| \qquad (4)$$

Where $(\Delta R/R)_X$ represents the error of reaction rate due to the uncertainty of the cross section X. The cross section library GICX40[5] which was used in this work was obtained by processing ENDF/B-III and -IV. Cross section uncertainties were estimated by making use of the reference[6] which keeps uncertainties for ENDF/B-IV. Estimated uncertainties are shown in Table 4.2. Values with the symbol o and those between symbols ∇ and Δ are directly obtained from the reference.[6]

Estimated errors of (n,p) reaction rates in the outer SCM are shown in Table 4.3. As for the ^{58}Ni(n,p) reaction rate, the overall error is about 50% in case of full correlation, and is about 35% in case of no correlation. The error due to the uncertainty of Fe total cross section is about 34% which is the largest. The error comprises about 70% of that due to the uncertainties of total cross sections of all elements in case of full correlation and nearly 100% in case of no correlation. As for the ^{54}Fe(n,p) reaction rate, the same tendency can be seen except that errors are larger than those for ^{58}Ni(n,p) reaction rate by about 20%. On the other hand, the uncertainty of ^{58}Ni(n,p) reaction cross section itself is about 5∿10%, and that of ^{54}Fe(n,p) is about 20%. As a whole, the error of the induced activity can be estimated as about 50∿70%.

The error of copper atomic displacement rate is about 65% in case of full correlation, and about 27% in case of no correlation. The error is the largest due to the uncertainly for the total cross section of Fe. But errors due to the uncertainties of tungsten are remarkably large. That results in the very large error due to the uncertainties of total cross sections in the case of full correlation.

Table 4.1 Comparison of $^{58}Ni(n,p)$ Reaction Sensitivities for the Total Cross Sections of JXFR Outer Constituent Elements Obtained from S_8 and S_{16} Perturbation Calculations

Zone	Region No.	Region	Sn and ratio	Element				
				^7Li	^{16}O	Cr	Fe	H
Blanket	4	Stainless Steel	S_8			-0.033	-0.120	
			S_{16}			-0.032	-0.115	
			S_8/S_{16}			1.040	1.043	
	5	Li_2O Pebble	S_8	-0.279	-0.194	-0.055	-0.204	
			S_{16}	-0.270	-0.188	-0.053	-0.197	
			S_8/S_{16}	1.033	1.032	1.034	1.036	
	6	Li_2O Block	S_8	-1.797	-1.190	-0.209	-0.793	
			S_{16}	-1.748	-1.157	-0.204	-0.771	
			S_8/S_{16}	1.028	1.028	1.025	1.028	
	7	S.S. Block	S_8			-0.544	-2.062	
			S_{16}			-0.532	-2.017	
			S_8/S_{16}			1.023	1.022	
	8	Stainless Steel	S_8			-0.134	-0.508	
			S_{16}			-0.132	-0.499	
			S_8/S_{16}			1.015	1.018	
Shield	10	H.C.+H_2O(B)	S_8		-2.636	-0.121	-4.512	-1.019
			S_{16}		-2.619	-0.121	-4.475	-1.008
			S_8/S_{16}		1.006	1.000	1.008	1.011
TFC	14	SCM	S_8				-0.414	
			S_{16}				-0.414	
			S_8/S_{16}				1.000	
Total			S_8	-2.076	-4.019	-1.097	-8.612	-1.019
			S_{16}	-2.018	-3.964	-1.074	-8.488	-1.008
			S_8/S_{16}	1.028	1.013	1.021	1.015	1.011

Table 4.2 Estimated Uncertainties of Total Cross Sections (%)

Group	Energy	H	^{6}Li	^{7}Li	^{16}O	^{27}Al	Cr	Fe	Ni	Cu	Mo	^{10}B	W
1	15.0-13.72 MeV	∘1	∘6	∘2	∘1	∘1	∘2	∇4	∘3	∘3	∇10	2	10
2	13.72-12.55	1	6	2	1	1	2	4	3	3	10	2	10
3	12.55-11.48	1	6	2	1	1	2	4	2	3	10	2	10
4	11.48-10.5	1	6	2	∘1	∘1	2	4	2	3	10	2	10
5	10.5 -9.31	1	5	2	1	1	∘2	4	∘2	∘3	10	2	10
6	9.31-8.26	1	5	2	1	1	2	4	2	3	10	2	10
7	8.26-7.33	1	5	2	∘1	∘1	2	Δ4	2	3	10	2	10
8	7.33-6.5	1	5	2	1	1	2	4	2	3	10	2	10
9	6.5 -5.76	1	4	2	1	1	2	4	2	3	Δ10	2	10
10	5.76-5.10	1	4	2	1	1	2	4	2	3	∇ 5	2	5
11	5.10-4.52	∘1	∘4	∘2	∘1	∘1	∘2	4	∘2	∘3	5	2	5
12	4.52-4.0	1	4	2	1	1	2	4	2	4	5	2	5
13	4.0 -3.16	1	6	3	1	1	2	4	2	5	5	2	5
14	3.16-2.5	1	∘8	∘3	∘1	∘1	∘2	4	∘2	∘5	5	2	5
15	2.5 -1.87	1	6	3	1	1	∘2	4	∘1.5	5	5	2	5
16	1.87-1.4	1	6	3	1	1	2	4	1.5	4	5	2	5
17	1.4 -1.06	1	5	3	1	1	2	4	1.5	3	5	2	5
18	1.06-0.8	∘1	∘5	∘3	∘1	∘1	∘2	4	∘1.5	∘2	5	2	5
19	0.8 -0.566	1	4	4	1	1	∇10	4	∇10	2	5	2	5
20	0.566-0.4	1	3	5	1	1	10	4	10	∘2	5	2	5
21	0.4 -0.283	1	∘2	∘5	1	1	10	4	10	2	5	2	5
22	0.283-0.2	1	2	5	1	1	10	4	10	4	5	2	5
23	0.2 -0.141	1	2	5	1	2	10	4	10	6	5	2	5
24	0.141-0.1	∘1	2	5	∘1	∘2	10	4	10	∘7	5	2	5
25	100 -46.5 keV	∘1	2	4	∘1	∘2	10	4	10	∘7	5	2	5
26	46.5-21.5	1	1.5	4	1	3	10	4	10	∘10	5	2	5
27	21.5-10.0	1	∘1.5	∘4	1	∘5	10	4	10	8	5	2	5
28	10.0-4.65	1	∘1.5	∘4	1	∘5	10	4	10	7	5	2	5
29	4.65-2.15	1	1.5	4	1	5	10	4	10	6	5	2	5
30,31	2.15-0.465	∘1	1.5	4	1	5	10	4	10	∘5	5	2	5
32∿41	465-0.215 eV	1	1.5	4	1	5	Δ10	4	Δ10	5	5	2	5
42	0.215-0.001	∘1	∘0.5	∘3	∘1	∘5	∘5	4	∘5	∘15	Δ5	2	5

N.B. Data with symbol ∘ and those between ∇ and Δ were obtained from USNDC-CTR-1

Table 4.3 Errors of (n,p) Reaction Rates in the Outer SCM Estimated from Cross Section Uncertainties and Calculated Sensitivities

Element	$^{58}Ni(n,p)$	$^{54}Fe(n,p)$
^{6}Li	0.89 %	1.08 %
^{7}Li	4.04 %	4.89 %
^{16}O	3.95 %	4.73 %
Fe	33.95 %	40.52 %
Cr	2.15 %	2.58 %
Ni	1.86 %	2.23 %
Mo	1.10 %	1.33 %
H	1.01 %	1.20 %
full correlation	49.0 %	58.6 %
no correlation	34.6 %	41.3 %

Table 4.4 Errors of Cu Displacement Rate in the Inner SCM Estimated from Cross Section Uncertainties and Calculated Sensitivities

Element	Cu Displacement
^{16}O	1.26 %
Fe	16.88 %
Cr	1.49 %
Ni	1.40 %
Mo	0.68 %
H	0.70 %
^{10}B	0.95 %
Al	0.30 %
Cu	0.15 %
^{182}W	11.00 %
^{183}W	5.95 %
^{184}W	12.62 %
^{186}W	11.39 %
full correlation	64.8 %
no correlation	27.2 %

5. CONCLUSION

A sensitivity study of neutronics characteristic quantities for the cross sections of JXFR was carried out with a corrected linear perturbation code SWANLAKE. According to the calculated results, an overall conclusions formerly reported turned out to be valid. But some of the contents are corrected since recalculated values differed a little from those of the former calculation. Here the conclusions obtained in this work are summarized.

(1) Sensitivities of the $^{6}Li(n,\alpha)$ reaction rate in the Li_2O pebble region are positive for total cross sections of constituent elements except ^{6}Li, since the increase of those cross sections other than ^{6}Li increases slow neutrons in the Li_2O pebble region.

(2) Sensitivities of $^{7}Li(n,n'\alpha)$ reaction rate in the Li_2O pebble region are fairly large for the total cross sections of Cr, Fe and Ni, since those elements have relatively large inelastic cross sections.

(3) Sensitivities of $^{6}Li(n,\alpha)$ reaction rate in the Li_2O block region are comparatively small except for the large negative value for ^{6}Li. Because the increase of the total cross section causes the increase of absorption of slow neutrons which cancels the effect of the increase of fast neutron slowing down.

(4) Sensitivities of the $^{7}Li(n,n'\alpha)$ reaction rate in the Li_2O block region have the similar tendency to those of the $^{7}Li(n,n'\alpha)$ reaction rates in the Li_2O pebble region. That is, all sensitivities are negative and large.

(5) Sensitivity of total tritium production reaction rate is negative for all the elements and especially large for the total cross section of ^{6}Li. Even the next largest sensitivities for the total cross sections of Fe and ^{16}O are only some 10% of the value for the total cross section of ^{6}Li. This is because the neutron absorption cross section of ^{6}Li is very large and comprises nearly all of the ^{6}Li total cross section in low energy region. But since the absorption is in reality the tritium producing (n,α) reaction, the net increase of the tritium production ratio is only 0.3% by the 1% increase of the total cross section of ^{6}Li.

(6) Sensitivities of (n,α) reaction rates in the outer part of the superconducting magnet are all negative since they are threshold reactions. In case of $^{58}Ni(n,p)$ reaction rate, the largest is for the total cross section of Fe, and sensitivities for the other elements are at most less than a half. $^{58}Ni(n,p)$ reaction rate decreases by 8.5% due to the 1% increase of Fe total cross section. Sensitivities of $^{54}Fe(n,p)$ reac-

tions have the similar tendencies, but are larger by about 20%.

(7) Sensitivity of atomic displacenent rate of Cu stabilizer in the inner part of the superconducting magnet is the largest for the total cross section of Fe. It is noted that sensitivities for tungsten isotopes are fairly large and the overall sensitivity for tungsten is nearly equal to that for Fe. Considering the smaller amount of tungsten present in comparison to iron, this shows tungsten is very effective for the shield material.

(8) Sensitivity change due to the difference of S_8 and S_{16} is small enough to justify the use of S_8 approximation for this type of analysis.

(9) The errors of reaction rates due to the uncertainties of cross sections were estimated. The error of $^{58}Ni(n,p)$ reaction rate is about $35 \sim 50\%$ and that of $^{54}Fe(n,p)$ reaction rate is about $40 \sim 60\%$. When the uncertainties of the (n,p) reaction cross sections themselves are considered, the errors of reaction rates are supposed to be about $50 \sim 70\%$. As for the copper atomic displacement rate, the error was estimated to be about $25 \sim 65\%$. In this case, the uncertainty of the displacement cross section itself is neglected. As a whole, it is supposed that uncertainties of reaction rates estimated in this work are not so large as to cause any serious problem in the nuclear design of the reactor.

REFERENCES

1) Michinori Yamauchi and Hiromasa Iida ; "Sensitivity Analysis of Neutronics Calculation in the Preliminary Design of Japan Experimental Fusion Reactor", JAERI-M 7915 (1978)(in Japanese)

2) Kiyoshi Sako, et al. ; "First Preliminary Design of an Experimental Fusion Reactor", JAERI-M 7300 (1977)(in Japanese)

3) D. E. Bartine, et al. ; "SWANLAKE, a computer Code Utilizing ANISN Radiation Transport Calculations for Cross Section Sensitivity Analysis", ORNL-TM-3809 (1973)

4) W. W. Engle, Jr. ; "A Users Manual for ANISN : a One Dimensional Discrete Ordinates Transport Code with Anisotropic Scattering", K-1693 (1967)

5) Yasushi Seki and Hiromasa Iida ; JAERI-M 8818 (1980)

6) D. Steiner (edited) ; " The status of Neutron-Induced Nuclear Data for Controlled Thermonuclear Research Applications", USNDC-CTR-1 (1974)

tions have the similar tendencies, but are larger by about 20%.

(7) Sensitivity of atomic displacenent rate of Cu stabilizer in the inner part of the superconducting magnet is the largest for the total cross section of Fe. It is noted that sensitivities for tungsten isotopes are fairly large and the overall sensitivity for tungsten is nearly equal to that for Fe. Considering the smaller amount of tungsten present in comparison to iron, this shows tungsten is very effective for the shield material.

(8) Sensitivity change due to the difference of S_8 and S_{16} is small enough to justify the use of S_8 approximation for this type of analysis.

(9) The errors of reaction rates due to the uncertainties of cross sections were estimated. The error of $^{58}Ni(n,p)$ reaction rate is about $35 \sim 50\%$ and that of $^{54}Fe(n,p)$ reaction rate is about $40 \sim 60\%$. When the uncertainties of the (n,p) reaction cross sections themselves are considered, the errors of reaction rates are supposed to be about $50 \sim 70\%$. As for the copper atomic displacement rate, the error was estimated to be about $25 \sim 65\%$. In this case, the uncertainty of the displacement cross section itself is neglected. As a whole, it is supposed that uncertainties of reaction rates estimated in this work are not so large as to cause any serious problem in the nuclear design of the reactor.

REFERENCES

1) Michinori Yamauchi and Hiromasa Iida ; "Sensitivity Analysis of Neutronics Calculation in the Preliminary Design of Japan Experimental Fusion Reactor", JAERI-M 7915 (1978)(in Japanese)

2) Kiyoshi Sako, et al. ; "First Preliminary Design of an Experimental Fusion Reactor", JAERI-M 7300 (1977)(in Japanese)

3) D. E. Bartine, et al. ; "SWANLAKE, a computer Code Utilizing ANISN Radiation Transport Calculations for Cross Section Sensitivity Analysis", ORNL-TM-3809 (1973)

4) W. W. Engle, Jr. ; "A Users Manual for ANISN : a One Dimensional Discrete Ordinates Transport Code with Anisotropic Scattering", K-1693 (1967)

5) Yasushi Seki and Hiromasa Iida ; JAERI-M 8818 (1980)

6) D. Steiner (edited) ; " The status of Neutron-Induced Nuclear Data for Controlled Thermonuclear Research Applications", USNDC-CTR-1 (1974)